Potentiation of the cystic fibrosis transmembrane conductance regulator Cl^- channel by ivacaftor is temperature-independent

Yiting Wang[1], Zhiwei Cai[1], Martin Gosling[2,3] and David N. Sheppard[1]

[1]School of Physiology, Pharmacology and Neuroscience, University of Bristol, Biomedical Sciences Building, University Walk, Bristol BS8 1TD, UK,

[2]Enterprise Therapeutics, Sussex Innovation Centre, University of Sussex, Science Park Square, Brighton BN1 9SB, UK

and

[3]Sussex Drug Discovery Centre, School of Life Sciences, University of Sussex, Brighton BN1 9QJ, UK

Running Title: Ivacaftor potentiation of CFTR is temperature-independent

Address Correspondence to: D.N. Sheppard, Ph.D.
University of Bristol
School of Physiology, Pharmacology and Neuroscience
Biomedical Sciences Building
University Walk
Bristol BS8 1TD
United Kingdom
Tel: +44 117 331 2290
Fax: +44 117 331 1889
E-mail: D.N.Sheppard@bristol.ac.uk

ABSTRACT

Ivacaftor is the first drug to target directly defects in the cystic fibrosis transmembrane conductance regulator (CFTR), which cause cystic fibrosis (CF). To understand better how ivacaftor potentiates CFTR channel gating, here we investigated the effects of temperature on its action. As a control, we studied the benzimidazolone UC_{CF}-853, which potentiates CFTR by a different mechanism. Using the patch-clamp technique and cells expressing recombinant CFTR, we studied the single-channel behavior of wild-type and F508del-CFTR, the most common CF mutation. Raising the temperature of the intracellular solution from 23 to 37 °C increased the frequency, but reduced the duration of wild-type and F508del-CFTR channel openings. While the open probability (P_o) of wild-type CFTR increased progressively as temperature was elevated, the relationship between P_o and temperature for F508del-CFTR was bell-shaped with a maximum P_o at ~30 °C. For wild-type CFTR and, to a greatly reduced extent, F508del-CFTR, the temperature-dependence of channel gating was asymmetric with the opening rate demonstrating greater temperature sensitivity than the closing rate. At all temperatures tested, ivacaftor and UC_{CF}-853 potentiated wild-type and F508del-CFTR. Strikingly, ivacaftor, but not UC_{CF}-853, abolished the asymmetric temperature-dependence of CFTR channel gating. At all temperatures tested, P_o values of wild-type CFTR in the presence of ivacaftor were approximately double those of F508del-CFTR, which were equivalent to or greater than those of wild-type CFTR at 37 °C in the absence of the drug. We conclude that the principal effect of ivacaftor is to promote channel opening to abolish the temperature-dependence of CFTR channel gating.

Key words: CFTR chloride ion channel / cystic fibrosis / F508del-CFTR / CFTR potentiation / ivacaftor (VX-770)

INTRODUCTION

The ATP-binding cassette (ABC) transporter cystic fibrosis transmembrane conductance regulator (CFTR; ABCC7) (33, 56) is a ligand-gated anion channel that plays a pivotal role in fluid and electrolyte transport across epithelia (28, 35). The importance of CFTR for epithelial physiology is highlighted by its dysfunction in the common, life-shortening genetic disease cystic fibrosis (55). To date, more than 2,000 mutations have been identified in the *CFTR* gene (http://www.genet.sickkids.on.ca/app), although most are very rare and not all cause disease. Among those mutations investigated, many disrupt CFTR expression and function by multiple mechanisms (70). This is best illustrated by F508del, the most common CF mutation, a temperature-sensitive folding defect, which not only disrupts the processing and intracellular transport of CFTR, but also destabilizes the protein at the plasma membrane and perturbs channel gating (19, 23, 24, 44).

To restore function to F508del-CFTR, combination therapy with small molecule CFTR correctors and potentiators is required (39, 50). Based on its mechanism of dysfunction (45), multiple CFTR correctors will likely be required to repair misfolding of nucleotide-binding domain 1 (NBD1) and restore correct domain assembly (52), leading to the delivery of F508del-CFTR to the plasma membrane. Once F508del-CFTR is activated by phosphorylated with protein kinase A (PKA), CFTR potentiators increase the frequency and/or duration of channel openings by modifying ATP-dependent or ATP-independent channel gating (15, 26, 37). To date, one CFTR potentiator, ivacaftor (VX-770; Vertex Pharmaceuticals) has been approved for patient use (54, 67). Ivacaftor treatment of CF patients with the gating mutation G551D achieves sustained, long-term clinical benefit, including slower lung function decline and improved nutrition (59). In combination with the CFTR corrector lumacaftor, ivacaftor also has clinical benefit for CF patients homozygous for

the F508del mutation, albeit the health improvements are less than for individuals with G551D treated with ivacaftor (68, 75). Nevertheless, laboratory studies suggest that lumacaftor-ivacaftor combination therapy is likely to be beneficial to CF patients with a variety of rare missense mutations in CFTR (10, 29, 32).

To understand better the action of ivacaftor, here we investigated the temperature-dependence of wild-type and F508del-CFTR potentiation by the small molecule. Using excised inside-out membrane patches from cells expressing recombinant CFTR, we studied single-channel behavior over the temperature range 23 to 37 °C. As a control, we studied the benzimidazolone UC_{CF}-853, which potentiates CFTR by a different mechanism to ivacaftor (2, 13, 39, 51). Our results demonstrated that ivacaftor, but not UC_{CF}-853, robustly potentiates CFTR at all temperatures tested, restoring wild-type levels of channel activity (as measured by open probability (P_o)) to F508del-CFTR. They also revealed that ivacaftor abolishes the temperature-dependence of CFTR channel gating.

METHODS

Cells and cell culture

We used C127 mouse mammary epithelial cells and baby hamster kidney (BHK) cells stably expressing wild-type human CFTR and the F508del mutation (27, 46). Cells were generous gifts of CR O'Riordan (Sanofi Genzyme; C127 cells) and MD Amaral (University of Lisboa; BHK cells). Cells were cultured and used as described previously (60, 61) with the exception that the plasma membrane expression of F508del-CFTR was rescued by either low temperature incubation (27 °C for 72 – 96 h) or treatment with lumacaftor (3 μM for 24 – 48 h at 37 °C). The single-channel behavior of human CFTR in excised membrane patches from

different mammalian cell lines is equivalent (wild-type CFTR, (18); F508del-CFTR, Y Wang, Z Cai and DN Sheppard, unpublished observation).

Patch-clamp experiments

CFTR Cl^- channels were recorded in excised inside-out membrane patches using Axopatch 200A and 200B patch-clamp amplifiers and pCLAMP software (all from Molecular Devices, San Jose, CA, USA) (61). The pipette (extracellular) solution contained (mM): 140 N-methyl-D-glucamine (NMDG), 140 aspartic acid, 5 $CaCl_2$, 2 $MgSO_4$ and 10 N-tris[Hydroxymethyl]methyl-2-aminoethanesulphonic acid (TES), adjusted to pH 7.3 with Tris ($[Cl^-]$, 10 mM). The bath (intracellular) solution contained (mM): 140 NMDG, 3 $MgCl_2$, 1 CsEGTA and 10 TES, adjusted to pH 7.3 with HCl ($[Cl^-]$, 147 mM; free $[Ca^{2+}]$, $< 10^{-8}$ M). Using a temperature-controlled microscope stage (Brook Industries, Lake Villa, IL, USA), the temperature of the bath solution was varied between 23 and 37 °C.

After excision of inside-out membrane patches, we added the catalytic subunit of protein kinase A (PKA; 75 nM) and ATP (1 mM) to the intracellular solution within 2 minutes of membrane patch excision to activate CFTR Cl^- channels. To minimize channel rundown, we added PKA (75 nM), but not protein phosphatase inhibitors, to all intracellular solutions, maintained millimolar concentrations of ATP (wild-type CFTR, $\geq$ 0.3 mM; F508del-CFTR, 1 mM) in the intracellular solution and clamped voltage at –50 mV. The effects of temperature on the single-channel behavior of CFTR were tested by increasing the temperature of the intracellular solution from 23 to 37 °C in 3 – 4 °C increments. Once channel activity stabilized at the new test temperature, we acquired 4 – 10 minutes of single-channel data before increasing further the temperature and repeating the acquisition of data. For wild-type CFTR, there was no difference in channel activity if temperature was decreased from 37 to 23 °C rather than increased from 23 to 37 °C. Because of the rundown of F508del-

CFTR at temperatures ≥ 27 °C, we only studied F508del-CFTR by increasing temperature from 23 to 37 °C.

The effects of CFTR potentiators were tested by addition to the intracellular solution in the continuous presence of ATP (1 mM [F508del-CFTR] or 0.3 mM [wild-type]) and PKA (75 nM). We reduced the ATP concentration when testing the effects of potentiators on wild-type CFTR to avoid P_o saturation in the presence of potentiators. For wild-type CFTR, after acquiring control recordings at temperatures between 23 – 37 °C, test potentiators were added to the intracellular solution and once channel activity was stable, we acquired data with the test potentiator over the same temperature range. For UC_{CF}-853, but not ivacaftor (77), after washing the potentiator from the recording chamber, control data were acquired again between 23 – 37 °C. Because of the rundown of F508del-CFTR Cl^- channels in excised membrane patches at temperatures ≥ 27 °C, data acquired under control conditions used different excised membranes patches from those used to acquire data in the presence of either UC_{CF}-853 or ivacaftor.

In this study, we used membrane patches containing ≤ 5 active channels (wild-type CFTR, number of active channels (N) ≤ 5; F508del-CFTR, N ≤ 5). To determine channel number, we used the maximum number of simultaneous channel openings observed during an experiment (16). To minimize errors, we used experimental conditions that robustly potentiate channel activity and verified that recordings were of sufficient length to ascertain the correct number of channels (72). Despite our precautions, we cannot exclude the possibility of unobserved F508del-CFTR Cl^- channels in excised membrane patches. Therefore, P_o values for F508del-CFTR might possibly be overestimated.

We recorded, filtered and digitized data as described previously (61). To measure single-channel current amplitude (i), Gaussian distributions were fit to current amplitude histograms. For P_o and burst analyses, lists of open- and closed-times were created using a half-amplitude crossing criterion for event detection and dwell-time histograms constructed as previously described (61); transitions < 1 ms were excluded from the analysis (eight-pole Bessel filter rise time ($T_{10\text{-}90}$) ~0.73 ms at f_c = 500 Hz). Histograms were fitted with one or more component exponential functions using the maximum likelihood method. For burst analysis, we used a t_c (the time that separates interburst closures from intraburst closures) determined from closed time histograms (wild-type CFTR: t = 23 °C, t_c = 22.5 ± 2.5 ms (n = 6); t = 37 °C, t_c = 15.3 ± 0.5 ms (n = 6); low temperature-rescued F508del-CFTR: t = 23 °C, t_c = 30.0 ± 2.3 ms (n = 4); t = 37 °C, t_c = 23.2 ± 1.6 ms (n = 4)) (16). The mean interburst interval (T_{IBI}) was calculated using Eq. 1 (see Ref. (16)):

$$P_o = T_b / (T_{MBD} + T_{IBI}), \qquad \text{(Eq. 1)}$$

where T_b = (mean burst duration) x (open probability within a burst). Mean burst duration (T_{MBD}) and open probability within a burst ($P_{o(burst)}$) were determined directly from experimental data using pCLAMP software. For wild-type CFTR, only membrane patches that contained a single active channel were used for burst analyses, whereas for F508del-CFTR, membrane patches contained no more than three active channels. We analyzed only bursts of F508del-CFTR single-channel openings with no superimposed openings that were separated from one another by a time interval > t_c.

To evaluate the temperature-dependence of current flow and channel gating, we calculated Q_{10} temperature coefficients using Eq. 2 (see Ref. (47)):

$$Q_{10} = (k_1 / k_2) (10 / (t_1 - t_2)) \qquad \text{(Eq. 2)}$$

where k_1 is the current amplitude or rate constant at temperature t_1, the higher temperature, and k_2 is the current amplitude or rate constant at temperature t_2, the lower temperature; all values of temperature for these calculations used the Kelvin scale. For the purpose of illustration, single-channel records were filtered at 500 Hz and digitized at 5 kHz before file size compression by 5-fold data reduction.

Reagents

The CFTR potentiator UC_{CF}-853 (Cystic Fibrosis Foundation Therapeutics (CFFT) CFTR Compound Program reference no. P4) (13) was a generous gift of RJ Bridges (Rosalind Franklin University of Medicine and Science, Chicago, IL, USA) and CFFT (Bethesda, MD, USA), while ivacaftor and lumacaftor were purchased from Selleck Chemicals (Stratech Scientific Ltd., Newmarket, UK). PKA purified from bovine heart was purchased from Calbiochem (Merck Chemicals Ltd., Nottingham, UK). All other chemicals were of reagent grade and supplied by the Sigma-Aldrich Company Ltd. (Gillingham, UK).

ATP was dissolved in intracellular solution, while ivacaftor, lumacaftor and UC_{CF}-853 were dissolved in DMSO. Stock solutions were stored at –20 °C except those of ATP, which were prepared freshly before each experiment. Immediately before use, stock solutions were diluted to final concentrations and, where necessary, the pH of the intracellular solution was re-adjusted to pH 7.3 to avoid pH-dependent changes in CFTR function (18). Precautions against light-sensitive reactions were observed when using CFTR modulators. DMSO was without effect on CFTR activity (61). On completion of experiments, the recording chamber was thoroughly cleaned before reuse (77).

Statistics

Data recording and analyses were randomized, but not blinded. Results are expressed as means ± SEM of n observations, but some group sizes were unequal due to technical difficulties with the acquisition of single-channel data. To test for differences between two groups of data acquired within the same experiment, we used Student's paired t-test. To test for differences between multiple groups of data, we used an analysis of variance (ANOVA) followed by post-hoc tests. All tests were performed using SigmaPlot^{TM} (version 13.0; Systat Software Inc., San Jose, CA, USA). Differences were considered statistically significant when $P < 0.05$. Data subjected to statistical analysis had n values ≥ 5 per group. In patch-clamp experiments, n represents the number of individual membrane patches obtained from different cells. To avoid pseudo-replication, all experiments were repeated at different times.

RESULTS

The single-channel activity of wild-type and F508del-CFTR is temperature-dependent

In this study, we investigated the temperature-dependence of wild-type and F508del-CFTR Cl^- channels and the effects of temperature on the action of the CFTR potentiators ivacaftor (67) and UC_{CF}-853 (P4; (13)). Using recombinant BHK and C127 cells and the excised inside-out configuration of the patch-clamp technique, we studied the single-channel behavior of CFTR between 23 and 37 °C by altering the temperature of the intracellular (bath) solution. For F508del-CFTR, all data were acquired while channel activity was stable prior to channel deactivation (49, 77).

Figure 1 shows representative recordings of wild-type and F508del-CFTR Cl^- channels following channel activation by PKA (75 nM) made in the presence of ATP (1 mM) in the intracellular solution, while Figure 2 quantifies the effects of temperature on current flow through open channels and the pattern of channel gating. To rescue the plasma membrane expression of F508del-CFTR, BHK cells expressing F508del-CFTR were either

incubated at 27 °C for 72 – 96 h or treated with the clinically-approved CFTR corrector lumacaftor (3 μM for 24 – 48 h at 37 °C). Consistent with previous results (for review, see Ref. (14)), Figures 1 and 2 demonstrate that the F508del mutation was without effect on current flow through CFTR Cl^- channels in the full-open state, but perturbed channel gating (i, $P = 0.9$; P_o, $P < 0.001$; one-way ANOVA with Dunnett's post-test). They also show that the single-channel behavior of F508del-CFTR rescued by low temperature or lumacaftor was equivalent. For both wild-type and F508del-CFTR, current flow through the full-open state increased 0.4-fold from 23 to 37 °C and Q_{10} temperature coefficient values were comparable (Fig. 2A and Table 1).

The gating behavior of wild-type CFTR is characterized by bursts of channel openings interrupted by brief, flickery closures separated by longer closures between bursts (Fig. 1A). Consistent with previous results (5, 47), Figure 1A demonstrates that increasing the temperature of the intracellular solution had a marked impact on the gating pattern of wild-type CFTR. As temperature rose from 23 to 37 °C, the frequency of channel openings increased (as interburst interval [IBI] decreased 6.4-fold), but their duration decreased (as mean burst duration [MBD] diminished 0.9-fold) with the result that P_o was enhanced 1.2-fold (Fig. 2B – D). At all temperatures tested, F508del-CFTR demonstrated a noticeably different pattern of channel gating compared to that of wild-type CFTR (Fig. 1). At 23 °C, the frequency of F508del-CFTR channel openings was reduced compared to those of wild-type, but their duration was increased, leading to a 2.8-fold lower P_o than that of wild-type CFTR (Fig. 2B – D). As temperature rose from 23 to 37 °C, the frequency of F508del-CFTR channel openings increased, but their duration decreased, such that at 37 °C, the MBD of F508del-CFTR was 0.3-fold shorter than that of wild-type CFTR and its IBI was 6.3-fold longer with the result that the P_o of F508del-CFTR was 10-fold lower than that of wild-type

CFTR (Fig. 2B – D). Consistent with previous results (42, 49), the data also show that there was no difference in the temperature-dependence of channel gating between F508del-CFTR Cl^- channels rescued by low temperature incubation or treatment with lumacaftor (Fig. 2C and D). Thus, at both 23 and 37 °C, bursts of F508del-CFTR channel openings were very infrequent compared to those of wild-type CFTR. However, at 23 °C openings of F508del-CFTR were greatly prolonged, whereas at 37 °C they were reduced in length compared to those of wild-type CFTR (Fig. 1).

Interestingly, wild-type and F508del-CFTR exhibited strikingly different relationships between temperature and P_o. For wild-type CFTR, P_o values increased progressively between 23 and 37 °C (Fig. 2B). By contrast, F508del-CFTR rescued by either low temperature or lumacaftor exhibited a bell-shaped relationship between temperature and P_o with values increasing to a maximum around 30 °C after which they decreased to approach those recorded at 23 °C (Fig. 2B). Consistent with previous results (47), wild-type CFTR exhibited asymmetric Q_{10} values for channel gating because the opening rate had ~3-fold greater temperature-dependence than the closing rate (Table 1). F508del-CFTR rescued by either low temperature or lumacaftor also had asymmetric Q_{10} values for channel gating, albeit the difference in temperature-dependence of opening and closing rates was much less marked and not statistically significant for VX-809-rescued F508del-CFTR ($P = 0.16$; Student's paired t-test) (Table 1).

Potentiation of wild-type and F508del-CFTR by UC_{CF}-853 is temperature-dependent

To investigate the effects of temperature on CFTR potentiation by small molecules, we selected for study ivacaftor (67) and UC_{CF}-853 (P4; (13)). Figure 3 shows representative recordings of wild-type and low temperature-rescued F508del-CFTR Cl^- channels following the acute addition of UC_{CF}-853 (10 μM) to the intracellular solution bathing excised

membrane patches acquired at temperatures between 23 and 37 °C, while Figure 4 quantifies the action of UC_{CF}-853 on current flow and channel gating. To avoid saturation of the wild-type CFTR response in the presence of UC_{CF}-853, we reduced the ATP concentration in the intracellular solution to 0.3 mM. At all temperatures tested, UC_{CF}-853 was without effect on current flow through wild-type and F508del-CFTR Cl^- channels in the full-open state (Figs. 3 and Fig. 4A and Table 1), albeit in these experiments there was a statistically significant difference in single-channel current amplitude between wild-type and low temperature-rescued F508del-CFTR ($P < 0.001$; one-way ANOVA with Dunnett's post-test) (Fig. 4A).

Figure 3 demonstrates that for both wild-type and low temperature-rescued F508del-CFTR UC_{CF}-853 (10 μM) altered the temperature-dependence of channel gating. At all temperatures tested, UC_{CF}-853 enhanced 0.5 – 0.6-fold the P_o of wild-type CFTR with the result that the relationship between P_o and temperature was unaltered, but shifted to higher P_o values (Fig. 4B). Similarly, for low temperature-rescued F508del-CFTR, UC_{CF}-853 elevated P_o values at all temperatures tested, but it also shifted the maximal P_o recorded for F508del-CFTR from ~30 °C to ~33 °C with the result that the bell-shaped relationship between temperature and P_o was displaced upwards and to the right. Burst analysis of wild-type CFTR channel gating demonstrated that at all temperatures tested, UC_{CF}-853 (10 μM) elicited similar increases in the frequency (by reducing IBI 2.4-fold at 23 ^oC and 0.5-fold at 37 ^oC) and duration (by increasing MBD 0.3-fold at 23 ^oC and 0.5-fold at 37 ^oC) of channel openings (Fig. 4C and D). By contrast, the UC_{CF}-853-dependent enhancement of low temperature-rescued F508del-CFTR channel gating was achieved by increased frequency of channel openings (23 °C, 1.7-fold; 37 °C, 1.3-fold) (Fig. 4D). Except at 23 °C where UC_{CF}-853 (10 μM) reduced MBD, the small molecule had little or no effect on the duration of F508del-CFTR channel openings (Fig. 4C). Interestingly, Table 1 reveals that UC_{CF}-853 accentuated

306 the asymmetry in Q_{10} values of channel gating for wild-type and F508del-CFTR by effects on
307 the temperature-dependence of the opening and closing rates.
308
309 **Ivacaftor potentiation of wild-type and F508del-CFTR is temperature-independent**
310 Next, we examined the temperature-dependence of CFTR potentiation by ivacaftor
311 (67). Figure 5 shows representative recordings of wild-type and low temperature-rescued
312 F508del-CFTR following acute addition of ivacaftor (10 μM) to the intracellular solution
313 acquired at the indicated temperatures and Figure 6 summary data from 4 – 7 experiments.
314 Like UC_{CF}-853 (Fig. 4A), ivacaftor did not alter current flow through wild-type and F508del-
315 CFTR Cl^- channels at each of the temperatures tested between 23 and 37 °C (Figs. 5 and 6A
316 and Table 1).
317
318 At all temperatures tested, ivacaftor robustly enhanced the P_o of wild-type and low
319 temperature-rescued F508del-CFTR (Fig. 6B). Strikingly, the drug eliminated the
320 temperature-dependence of P_o for wild-type and F508del-CFTR Cl^- channels with the result
321 that at all temperatures tested, P_o values of acutely potentiated wild-type CFTR were double
322 those of acutely potentiated low temperature-rescued F508del-CFTR (Fig. 6B). At 37 °C, the
323 P_o value of low temperature-rescued F508del-CFTR was the same as that of wild-type CFTR
324 in the absence of the drug, whereas at 23 °C, it was 0.4-fold larger than that of the wild-type
325 CFTR control (Fig. 6B). Burst analysis revealed that ivacaftor acutely potentiated wild-type
326 CFTR by increasing the frequency (by reducing IBI) and duration (by prolonging MBD) of
327 channel openings (Fig. 6C and D). The data also reveal that the changes in MBD and IBI of
328 wild-type CFTR were most marked at 23 °C, where MBD increased 1.9-fold and IBI
329 decreased 3-fold (Fig. 6C and D). For low temperature-rescued F508del-CFTR, the major
330 effect of ivacaftor was on the frequency of channel openings (by reducing IBI 4.7-fold at 23

°C and 2.1-fold at 37 °C) (Fig. 6D). However, at all temperatures tested ivacaftor prolonged channel openings by increasing MBD (Fig. 6C). Consistent with the drug's effects on P_o, analysis of Q_{10} values demonstrates that ivacaftor abolished the asymmetric temperature-dependence of channel gating (Table 1). For both wild-type and F508del-CFTR, the temperature-dependence of the opening and closing rates were equivalent in the presence of ivacaftor (Table 1).

To investigate further the action of ivacaftor, we studied the effects of nanomolar concentrations of ivacaftor and examined the consequences of treating lumacaftor-rescued F508del-CFTR Cl^- channels chronically with the drug. Because micromolar concentrations of ivacaftor destabilise F508del-CFTR (20, 48), we repeated our studies of wild-type CFTR using ivacaftor (100 nM). Figure 7 shows representative recordings acquired at the indicated temperatures for low temperature-rescued F508del-CFTR acutely treated with ivacaftor (100 nM) and summary data from 3 – 5 experiments. Comparison of single-channel records suggests that reducing the ivacaftor concentration was without effect on current flow through open channels, but modified channel gating (Figs. 5 – 7). An analysis of bursts revealed that there was little or no change in MBD on reducing the ivacaftor concentration from 10 μM to 100 nM (Fig. 7D). By contrast, IBI values were noticeably shorter with ivacaftor (100 nM), although the temperature-dependence of IBI resembled that observed using ivacaftor (10 μM) (Fig. 7E). As a result, ivacaftor (100 nM) also abolished the asymmetric temperature-dependence of channel gating (Table 1), while P_o values were temperature-independent and 0.5-fold greater than those determined using ivacaftor (10 μM) ($P = 0.14$; one-way ANOVA with Dunnett's post-test) (Fig. 7C).

Chronic ivacaftor treatment accentuates the thermoinstability of F508del-CFTR rescued by lumacaftor (21, 71). We therefore studied the temperature-dependence of lumacaftor-rescued F508del-CFTR treated chronically with ivacaftor at 27 and 37 °C only. Figure 8 shows representative recordings and Figure 9 summary data from 5 – 10 experiments. Chronic treatment with ivacaftor (1 μM) caused a small, albeit statistically significant (27 ^{o}C, $P < 0.0001$; 37 ^{o}C, $P < 0.05$) reduction in current flow through fully open F508del-CFTR Cl^- channels at both 27 and 37 °C (Fig. 9A). By contrast, at both temperatures, the P_o of lumacaftor-rescued F508del-CFTR-treated chronically with ivacaftor exceeded that of low temperature-rescued F508del-CFTR treated acutely with the drug (Fig. 9B). As for acute treatment with the drug, the major effect of chronic ivacaftor treatment was to increase greatly the frequency of F508del-CFTR channel openings, although the drug also caused some prolongation of channel openings (Fig. 9C and D). Thus, through effects on the frequency and duration of channel openings, ivacaftor eliminates the temperature-dependence of CFTR activity.

DISCUSSION

This study investigated the temperature dependence of CFTR potentiation by ivacaftor and UC_{CF}-853. At all temperatures tested, ivacaftor and UC_{CF}-853 potentiated CFTR channel gating. However, potentiation by ivacaftor, but not UC_{CF}-853, abolished the temperature-dependence of channel gating for both wild-type and F508del-CFTR.

The temperature-dependence of current flow through wild-type CFTR resembles that of different ion channels, whereas the temperature-dependence of CFTR channel gating is greater than that of many different ion channels, but is similar to that of ATPases (for review, see Ref. (47)). Our own analyses of the temperature-dependence of wild-type CFTR concur

with the findings of Mathews et al. (47) and show that the opening rate of wild-type CFTR is ~3-fold more temperature-dependent than the closing rate. Of note, Mathews et al. (47) interpreted the asymmetric temperature-dependence of channel opening and closing as potential support for a cyclic gating scheme. Building on these and other data (e.g. (73, 74)), Csanády et al. (22) used the temperature-dependence of channel gating to propose an energetic profile for the irreversible gating cycle of CFTR. The authors' analysis argues that channel opening proceeds as a wave of conformational change, which is initiated by formation of an ATP-bound NBD1:NBD2 dimer and then sweeps to the membrane-spanning domains (MSDs), leading to opening of the channel pore. By applying rate-equilibrium free-energy relationship analysis to the hydrolysis-deficient CFTR mutant D1370N, Sorum et al. (62) verified this model of channel opening and identified the interface between the NBDs and the MSDs as an energetic barrier to channel opening. Interestingly, the temperature-dependence of channel closure suggests that large scale protein movements are not required to close the CFTR pore (22). Instead, the hydrolysis of a single chemical bond in ATP bound at ATP-binding site 2 drives pore closure, which precedes partial disassembly of the NBD1:NBD2 dimer interface (22, 63, 65).

Analysis of the temperature-dependence of F508del-CFTR reveals that the mutant protein exhibits marked thermoinstability in excised membrane patches and planar lipid bilayers (3, 43, 49, 76). The irreversible loss of F508del-CFTR channel activity at 37 °C in the continuous presence of PKA and ATP involves both changes in channel gating and current flow through open channels (3, 49). Because revertant (second site) mutations in *cis* with F508del prevent the deactivation of F508del-CFTR Cl^- channels (4, 43, 76), the thermoinstability of F508del-CFTR is likely a consequence of structural defects not loss of anchoring to CFTR-interacting proteins (31). Previous studies of the temperature dependence

of F508del-CFTR prior to channel deactivation using the planar lipid bilayer technique show that F508del-CFTR activity declines with increasing temperature (4, 8). The present studies were performed under different experimental conditions using excised membrane patches. They reveal that prior to channel deactivation, F508del-CFTR has a bell-shaped relationship between temperature and P_o with a maximum P_o at ~30 °C, which is modulated by CFTR potentiators. As for wild-type CFTR, the temperature-dependence of F508del-CFTR channel gating was asymmetric, albeit the difference between the opening and closing rates was greatly reduced and closure of the mutant channel required greater energy than wild-type CFTR. This surprising result contrasts with previous work which shows that the F508del mutation destabilizes the NBD1:NBD2 dimer (38).

Strikingly, the present results demonstrate that ivacaftor, but not UC_{CF}-853, eliminated the temperature-dependence of CFTR channel gating. In the presence of ivacaftor, P_o values did not alter with increasing temperature and the temperature-dependence of channel gating was lost. Because the channel opening rate shows greatest temperature sensitivity (47, present study), the data suggest that the principal effect of ivacaftor is to promote channel opening, particularly at temperatures ≤ 30 °C. Integrating these data with biochemical and structural data, which demonstrated that ivacaftor reduces thermal stability (12, 49) and increases conformational flexibility (21), argues that ivacaftor exerts its effects by destabilizing a closed channel conformation. In addition, loss of the temperature-dependence of channel gating suggests that ivacaftor might modify the irreversible cyclic gating scheme of CFTR to favor a reversible one. Although this idea is only speculation, analysis of ivacaftor's action using the energetic coupling model of CFTR gating (40), demonstrated that the drug promotes gating transitions that favor channel open states (37) as the present data

confirm. Of note, this analysis also provided an explanation for ivacaftor's ability to promote both ATP-dependent and ATP-independent channel gating (26, 37).

The robust potentiation of CFTR channel gating achieved by ivacaftor confers wild-type levels of channel activity (as measured by P_o) on F508del-CFTR and other CF mutants once delivered to the plasma membrane ((58, 67, 77, 79); present study). However, it is important to emphasize that ivacaftor accelerates the deactivation of most, but not all, F508del-CFTR Cl^- channels delivered to the plasma membrane by either low temperature or lumacaftor (21, 49, 71). In contrast to ivacaftor, at physiological temperatures, the benzimidazolone UC_{CF}-853 did not confer wild-type levels of channel activity on low temperature-rescued F508del-CFTR Cl^- channels. This distinction between ivacaftor and UC_{CF}-853 might reflect the different potency and efficacy of a clinically-licensed drug and a screening hit (13, 67). Alternatively, it might reflect their diverse mechanisms of action. Al-Nakkash et al. (2) demonstrated that the benzimidazolones NS004 and NS1619 potentiate CFTR by a mechanism resembling that of genistein (34). Using the ATP-driven NBD dimerization model of CFTR channel gating (73, 74), Ai et al. (1) speculated that genistein might bind at the NBD1:NBD2 dimer interface and accelerate channel opening by lowering the free energy of the transition state, while slowing channel closure by stabilizing the binding of ATP at ATP-binding sites 1 and 2. Consistent with these ideas, Moran et al. (51) used virtual ligand docking with a molecular model of the NBD1:NBD2 dimer to suggest that genistein and UC_{CF}-853 bind at the dimer interface.

To date, the binding site for ivacaftor has not been identified. However, several lines of evidence argue that it is distinct from that of genistein, UC_{CF}-853 and other potentiators that interact with the NBDs (1, 2, 16). First, ivacaftor's ability to potentiate ATP-independent gating, the drug's lack of effect on the ATPase activity of CFTR and its potentiation of a

CFTR construct missing NBD2 (26, 37, 78), argue persuasively that it does not interact with the ATP-binding sites. Second, ivacaftor potentiation of ΔR-CFTR, which lacks a large portion of the R domain (residues 634 – 836; (37)), demonstrates that the drug does not bind the R domain. Third, the accumulation of ivacaftor in the inner leaflet of the lipid bilayer and the reduced sensitivity of some CF mutations in the MSDs to potentiation by ivacaftor (9, 69), suggests that ivacaftor might exert its effects by interacting with the MSDs. Such a site of action supports the drug's effects on the kinetics of channel gating (37). Using hydrogen/deuterium exchange mass spectroscopy, Byrnes et al. (12) investigated ivacaftor binding to a human CFTR construct with thermostabilizing mutations that themselves modify CFTR channel gating (4, 57). Intriguingly, ivacaftor bound to multiple sites on this CFTR construct, including the Lasso motif (80), transmembrane segment 2 in MSD1, the coupling helices of intracellular loops 1, 3 and 4 and NBD2 with tightest binding located at the MSD2-NBD1 and MSD2-NBD2 interfaces (12). These data suggest that ivacaftor might bind near F508 in a region overlapping the small molecule-binding sites identified by Kalid et al. (41) at the interface of the NBDs with the MSDs. Nevertheless, virtual ligand docking data suggest other potential binding sites for ivacaftor including one at the NBD1:NBD2 interface in the partially unfolded structure of F508del-CFTR (71).

Most studies of CFTR function using the patch-clamp technique are conducted at room temperature (~23 °C). An advantage of working at room temperature is that the kinetics of CFTR channel gating are slowed, permitting the resolution of short-lived gating transitions that are challenging to detect at 37 °C (e.g. (36)). However, studying mutant CFTR at room temperature might preclude full understanding of the mechanism of CFTR dysfunction. For example, channel deactivation or rundown, one measure of the plasma membrane instability of CF mutants, is best observed at temperatures ≥ 30 °C, (3, 43, 49, 76, 77). Moreover, the

present results show that at 23 °C, the rate of F508del-CFTR channel closure is markedly slowed compared to wild-type CFTR, whereas at 37 °C, it is equivalent to that of wild-type CFTR or even faster, hinting at instability of the open channel conformation, possibly the interaction of ATP with ATP-binding site 2 (38, 74). Although we have not evaluated directly the temperature-dependence of other CF mutants, comparison of our own data with those of other investigators suggests that temperature influences their gating behavior (e.g. N1303K-CFTR (25, 32)). Differences in temperature also likely explain inconsistencies in the published literature on CFTR modulators. Previous work showed that the non-hydrolysable ATP analogue AMP-PNP locked CFTR Cl^- channels in the open configuration at temperatures ≤ 30 °C, but at temperatures ≥ 30 °C, locking events were seldom observed, if at all (17, 47). Future studies of new CFTR potentiators should include assessment of their temperature-dependence to assist the identification of small molecules with therapeutic potential.

Although body temperature is normally tightly controlled, fluctuations occur during fever and chills, symptoms associated with pulmonary exacerbations in CF (30). Previous work suggests that body temperature and metabolic activity might influence CFTR behavior (11). This idea might explain the different effects of temperature on the single-channel activity of human CFTR observed in the present study and the CFTR-mediated Cl^- conductance of intact microperfused human sweat ducts, which achieved maximal activity around 30 °C (53). Alternatively, or in addition, differences in the experimental conditions used to study recombinant CFTR in excised membrane patches and native CFTR in intact sweat ducts might provide an explanation. Because the cellular ATP concentration exceeds the K_m (substrate concentration required for half maximal activity) for CFTR regulation by ATP and inhibition by ADP is likely to be weak at cellular concentrations (6, 7, 64), the

balance of protein kinase and phosphatase activity predominantly controls CFTR activity *in vivo* (28). This highlights the therapeutic potential of small molecules that promote the phosphorylation of CFTR by PKA (e.g. RPL554; (66)). Importantly, following CFTR phosphorylation by PKA, ivacaftor potentiates both ATP-dependent and ATP-independent CFTR channel gating (26, 37), highlighting its value in the treatment of CF (54, 59).

In conclusion, wild-type and, to a much reduced extent, F508del-CFTR demonstrate asymmetric temperature-dependence of channel gating with the opening rate exhibiting greater temperature sensitivity than the closing rate. Ivacaftor robustly potentiates CFTR at all temperatures tested, restoring wild-type levels of channel activity to F508del-CFTR and abolishing the temperature-dependence of CFTR channel gating. Thus, temperature has the potential to influence markedly the gating pattern of CF mutants and the action of small molecule CFTR modulators.

AUTHOR CONTRIBUTIONS

Conception and design of the experiments: D.N.S.; performed the research: Y.W.; analysis and interpretation of data: Y.W., Z.C., M.G. and D.N.S.; drafting the article or revising it critically for important intellectual content: Y.W and D.N.S. All authors approved the final version of the manuscript.

CONFLICT OF INTEREST

M.G. is Chief Scientific Officer of Enterprise Therapeutics. The other authors declare that they have no conflicts of interest with the contents of this article.

ACKNOWLEDGEMENTS

We thank MD Amaral, CR O'Riordan, RJ Bridges and CFFT for generous gifts of recombinant cells and the small molecule UC_{CF}-853 (P4). We are very grateful to our laboratory colleagues for valuable discussions and assistance. This work was funded by Cystic Fibrosis Foundation Therapeutics and the Cystic Fibrosis Trust. YW was supported by a scholarship from Beijing Sun-Hope Intellectual Property Ltd.

REFERENCES

1. **Ai T, Bompadre SG, Wang X, Hu S, Li M, Hwang T-C.** Capsaicin potentiates wild-type and mutant cystic fibrosis transmembrane conductance regulator chloride-channel currents. *Mol Pharmacol* 65: 1415-1426, 2004.

2. **Al-Nakkash L, Hu S, Li M, Hwang T-C.** A common mechanism for cystic fibrosis transmembrane conductance regulator protein activation by genistein and benzimidazolone analogs. *J Pharmacol Exp Ther* 296: 464-472, 2001.

3. **Aleksandrov AA, Kota P, Aleksandrov LA, He L, Jensen T, Cui L, Gentzsch M, Dokholyan NV, Riordan JR.** Regulatory insertion removal restores maturation, stability and function of ΔF508 CFTR. *J Mol Biol* 401: 194-210, 2010.

4. **Aleksandrov AA, Kota P, Cui L, Jensen T, Alekseev AE, Reyes S, He L, Gentzsch M, Aleksandrov LA, Dokholyan NV, Riordan JR.** Allosteric modulation balances thermodynamic stability and restores function of ΔF508 CFTR. *J Mol Biol* 419: 41-60, 2012.

5. **Aleksandrov AA, Riordan JR.** Regulation of CFTR ion channel gating by MgATP. *FEBS Lett* 431: 97-101, 1998.

6. **Anderson MP, Berger HA, Rich DP, Gregory RJ, Smith AE, Welsh MJ.** Nucleoside triphosphates are required to open the CFTR chloride channel. *Cell* 67: 775-784, 1991.

7. **Anderson MP, Welsh MJ.** Regulation by ATP and ADP of CFTR chloride channels that contain mutant nucleotide-binding domains. *Science* 257: 1701-1704, 1992.

8. **Bagdany M, Veit G, Fukuda R, Avramescu RG, Okiyoneda T, Baaklini I, Singh J, Sovak G, Xu H, Apaja PM, Sattin S, Beitel LK, Roldan A, Colombo G, Balch W, Young JC, Lukacs GL.** Chaperones rescue the energetic landscape of mutant CFTR at single molecule and in cell. *Nat Commun* 8: 398, 2017.

9. **Baroni D, Zegarra-Moran O, Svensson A, Moran O.** Direct interaction of a CFTR potentiator and a CFTR corrector with phospholipid bilayers. *Eur Biophys J* 43: 341-346, 2014.

10. **Birket SE, Chu KK, Houser GH, Liu L, Fernandez CM, Solomon GM, Lin V, Shastry S, Mazur M, Sloane PA, Hanes J, Grizzle WE, Sorscher EJ, Tearney GJ, Rowe SM.** Combination therapy with cystic fibrosis transmembrane conductance regulator modulators augment the airway functional microanatomy. *Am J Physiol Lung Cell Mol Physiol* 310: L928-L939, 2016.

11. **Bose SJ, Scott-Ward TS, Cai Z, Sheppard DN.** Exploiting species differences to understand the CFTR Cl^- channel. *Biochem Soc Trans* 43: 975-982, 2015.

12. **Byrnes LJ, Xu Y, Qiu X, Hall JD, West, GM.** Sites associated with Kalydeco binding on human cystic fibrosis transmembrane conductance regulator revealed by hydrogen/deuterium exchange. *Sci Rep* 8: 4664, 2018.

13. **Caci E, Folli C, Zegarra-Moran O, Ma T, Springsteel MF, Sammelson RE, Nantz MH, Kurth MJ, Verkman AS, Galietta LJV.** CFTR activation in human bronchial epithelial cells by novel benzoflavone and benzimidazolone compounds. *Am J Physiol Lung Cell Mol Physiol* 285: L180-L188, 2003.

14. **Cai Z-W, Liu J, Li H-Y, Sheppard DN.** Targeting F508del-CFTR to develop rational new therapies for cystic fibrosis. *Acta Pharmacol Sin* 32: 693-701, 2011.

15. **Cai Z, Sheppard DN.** Phloxine B interacts with the cystic fibrosis transmembrane conductance regulator at multiple sites to modulate channel activity. *J Biol Chem* 277: 19546-19553, 2002.

16. **Cai Z, Taddei A, Sheppard DN.** Differential sensitivity of the cystic fibrosis (CF)-associated mutants G551D and G1349D to potentiators of the cystic fibrosis transmembrane conductance regulator (CFTR) Cl^- channel. *J Biol Chem* 281: 1970-1977, 2006.

17. **Carson MR, Travis SM, Welsh MJ.** The two nucleotide-binding domains of cystic fibrosis transmembrane conductance regulator (CFTR) have distinct functions in controlling channel activity. *J Biol Chem* 270: 1711-1717, 1995.

18. **Chen J-H, Cai Z, Sheppard DN.** Direct sensing of intracellular pH by the cystic fibrosis transmembrane conductance regulator (CFTR) Cl^- channel. *J Biol Chem* 284: 35495-35506, 2009.

19. **Cheng SH, Gregory RJ, Marshall J, Paul S, Souza DW, White GA, O'Riordan CR, Smith AE.** Defective intracellular transport and processing of CFTR is the molecular basis of most cystic fibrosis. *Cell* 63: 827-834, 1990.

20. **Chin S, Hung M, Won A, Wu Y-S, Ahmadi S, Yang D, Elmallah S, Toutah K, Hamilton CM, Young RN, Viirre RD, Yip CM, Bear CE.** Lipophilicity of the cystic fibrosis drug, ivacaftor (VX-770), and its destabilizing effect on the major CF-causing mutation: F508del. *Mol Pharmacol* 94: 917-925, 2018.

21. **Cholon DM, Quinney NL, Fulcher ML, Esther CR Jr, Das J, Dokholyan NV, Randell SH, Boucher RC, Gentzsch M.** Potentiator ivacaftor abrogates pharmacological correction of ΔF508 CFTR in cystic fibrosis. *Sci Transl Med* 6: 246ra96, 2014.

22. **Csanády L, Nairn AC, Gadsby DC.** Thermodynamics of CFTR channel gating: a spreading conformational change initiates an irreversible gating cycle. *J Gen Physiol* 128: 523-533, 2006.

23. **Dalemans W, Barbry P, Champigny G, Jallat S, Dott K, Dreyer D, Crystal RG, Pavirani A, Lecocq J-P, Lazdunski M.** Altered chloride ion channel kinetics associated with the ΔF508 cystic fibrosis mutation. *Nature* 354: 526-528, 1991.

24. **Denning GM, Anderson MP, Amara JF, Marshall J, Smith AE, Welsh MJ.** Processing of mutant cystic fibrosis transmembrane conductance regulator is temperature-sensitive. *Nature* 358: 761-764, 1992.

25. **DeStefano, S., Gees, M., and Hwang, T.-C.** Physiological and pharmacological characterization of the N1303K mutant CFTR. *J Cyst Fibros* 2018; doi: 10.1016/j.jcf.2018.05.011. [Epub ahead of print].

26. **Eckford PDW, Li C, Ramjeesingh M, Bear CE.** Cystic fibrosis transmembrane conductance regulator (CFTR) potentiator VX-770 (ivacaftor) opens the defective channel gate of mutant CFTR in a phosphorylation-dependent but ATP-independent manner. *J Biol Chem* 287: 36639-36649, 2012.

27. **Farinha CM, Nogueira P, Mendes F, Penque D, Amaral MD.** The human DnaJ homologue (Hdj)-1/heat-shock protein (Hsp) 40 co-chaperone is required for the *in vivo* stabilization of the cystic fibrosis transmembrane conductance regulator by Hsp70. *Biochem J* 366: 797-806, 2002.

28. **Frizzell RA, Hanrahan JW.** Physiology of epithelial chloride and fluid secretion. *Cold Spring Harb Perspect Med* 2: a009563, 2012.

29. **Gentzsch M, Ren HY, Houck SA, Quinney NL, Cholon DM, Sopha P, Chaudhry IG, Das J, Dokholyan NV, Randell SH, Cyr DM.** Restoration of R117H CFTR folding and function in human airway cells through combination treatment with VX-809 and VX-770. *Am J Physiol Lung Cell Mol Physiol* 311: L550-L559, 2016.

30. **Goss CH, Edwards TC, Ramsey BW, Aitken ML, Patrick DL.** Patient-reported respiratory symptoms in cystic fibrosis. *J Cyst Fibros* 8 :245-252, 2009.

31. **Guggino WB, Stanton BA.** New insights into cystic fibrosis: molecular switches that regulate CFTR. *Nat Rev Mol Cell Biol* 7: 426-436, 2006.

32. **Han ST, Rab A, Pellicore MJ, Davis EF, McCague AF, Evans TA, Joynt AT, Lu Z, Cai Z, Raraigh KS, Hong J, Sheppard DN, Sorscher EJ, Cutting GR.** Residual function of cystic fibrosis mutants predicts response to small molecule CFTR modulators. *JCI Insight* 3: e121159, 2018.

33. **Holland IB, Cole SPC, Kuchler K, Higgins CF**. *ABC Proteins: from bacteria to man*. London: Academic Press, 2003.

34. **Hwang T-C, Sheppard DN.** Molecular pharmacology of the CFTR Cl^- channel. *Trends Pharmacol Sci* 20: 448-453, 1999.

35. **Hwang T-C, Yeh J-T, Zhang J, Yu H-I, Destefano S.** Structural mechanisms of CFTR function and dysfunction. *J Gen Physiol* 150: 539-570, 2018.

36. **Ishihara H, Welsh MJ.** Block by MOPS reveals a conformation change in the CFTR pore produced by ATP hydrolysis. *Am J Physiol Cell Physiol* 273: C1278-C1289, 1997.

37. **Jih K-Y, Hwang T-C.** Vx-770 potentiates CFTR function by promoting decoupling between the gating cycle and ATP hydrolysis cycle. *Proc Natl Acad Sci USA* 110: 4404-4409, 2013.

38. **Jih K-Y, Li M, Hwang T-C, Bompadre SG.** The most common cystic fibrosis-associated mutation destabilizes the dimeric state of the nucleotide-binding domains of CFTR. *J Physiol* 589: 2719-2731, 2011.

39. **Jih K-Y, Lin W-Y, Sohma Y, Hwang T-C.** CFTR potentiators: from bench to bedside. *Curr Opin Pharmacol* 34: 98-104, 2017.

40. **Jih K-Y, Sohma Y, Hwang T-C.** Nonintegral stoichiometry in CFTR gating revealed by a pore-lining mutation. *J Gen Physiol* 140: 347-359, 2012.

41. **Kalid O, Mense M, Fischman S, Shitrit A, Bihler H, Ben-Zeev E, Schutz N, Pedemonte N, Thomas PJ, Bridges RJ, Wetmore DR, Marantz Y, Senderowitz H.** Small molecule correctors of F508del-CFTR discovered by structure-based virtual screening. *J Comput Aided Mol Des* 24: 971-991, 2010.

42. **Kopeikin Z, Yuksek Z, Yang H-Y, Bompadre SG.** Combined effects of VX-770 and VX-809 on several functional abnormalities of F508del-CFTR channels. *J Cyst Fibros* 13: 508-514, 2014.

43. **Liu X, O'Donnell N, Landstrom A, Skach WR, Dawson DC.** Thermal instability of ΔF508 cystic fibrosis transmembrane conductance regulator (CFTR) channel function: protection by single suppressor mutations and inhibiting channel activity. *Biochemistry* 51: 5113-5124, 2012.

44. **Lukacs GL, Chang X-B, Bear C, Kartner N, Mohamed A, Riordan JR, Grinstein S.** The ΔF508 mutation decreases the stability of cystic fibrosis transmembrane conductance regulator in the plasma membrane: determination of functional half-lives on transfected cells. *J Biol Chem* 268: 21592-21598, 1993.

45. **Lukacs, GL, Verkman AS.** CFTR: folding, misfolding and correcting the ΔF508 conformational defect. *Trends Mol Med* 18: 81-91, 2012.

46. **Marshall J, Fang S, Ostedgaard LS, O'Riordan CR, Ferrara D, Amara JF, Hoppe H IV, Scheule RK, Welsh MJ, Smith AE, Cheng SH.** Stoichiometry of recombinant cystic fibrosis transmembrane conductance regulator in epithelial cells and its functional reconstitution into cells *in vitro*. *J Biol Chem* 269: 2987-2995, 1994.

47. **Mathews CJ, Tabcharani JA, Hanrahan JW.** The CFTR chloride channel: nucleotide interactions and temperature-dependent gating. *J Membr Biol* 163: 55-66, 1998.

48. **Matthes E, Goepp J, Carlile GW, Luo Y, Dejgaard K, Billet A, Robert R, Thomas DY, Hanrahan JW.** Low free drug concentration prevents inhibition of F508del CFTR functional expression by the potentiator VX-770 (ivacaftor). *Br J Pharmacol* 173: 459-470, 2016.

49. **Meng X, Wang Y, Wang X, Wrennall JA, Rimington TL, Li H, Cai Z, Ford RC, Sheppard DN.** Two small molecules restore stability to a sub-population of the cystic fibrosis transmembrane conductance regulator with the predominant disease-causing mutation. *J Biol Chem* 292: 3706-3719, 2017.

50. **Mijnders M, Kleizen B, Braakman I.** Correcting CFTR folding defects by small-molecule correctors to cure cystic fibrosis. *Curr Opin Pharmacol* 34: 83-90, 2017.

51. **Moran O, Galietta LJV, Zegarra-Moran O.** Binding site of activators of the cystic fibrosis transmembrane conductance regulator in the nucleotide binding domains. *Cell Mol Life Sci* 62: 446-460, 2005.

52. **Okiyoneda T, Veit G, Dekkers JF, Bagdany M, Soya N, Xu H, Roldan A, Verkman AS, Kurth M, Simon A, Hegedus T, Beekman JM, Lukacs GL.** Mechanism-based corrector combination restores ΔF508-CFTR folding and function. *Nat Chem Biol* 9: 444-454, 2013.

53. **Quinton PM.** Missing Cl conductance in cystic fibrosis. *Am J Physiol Cell Physiol* 251: C649-C652, 1986.

54. **Ramsey BW, Davies J, McElvaney NG, Tullis E, Bell SC, Dřevínek P, Griese M, McKone EF, Wainwright CE, Konstan MW, Moss R, Ratjen F, Sermet-Gaudelus I, Rowe SM, Dong Q, Rodriguez S, Yen K, Ordoñez C, Elborn JS, VX08-770-102 Study Group.** A CFTR potentiator in patients with cystic fibrosis and the *G551D* mutation. *N Engl J Med* 365: 1663-1671, 2011.

55. **Ratjen F, Bell SC, Rowe SM, Goss CH, Quittner AL, Bush A.** Cystic fibrosis. *Nat Rev Dis Primers* 1: 15010. 2015.

56. **Riordan JR, Rommens JM, Kerem B-S, Alon N, Rozmahel R, Grzelczak Z, Zielenski J, Lok S, Plavsic N, Chou J-L, Drumm ML, Iannuzzi MC, Collins FS, Tsui L-C.** Identification of the cystic fibrosis gene: cloning and characterization of complementary DNA. *Science* 245: 1066-1073. 1989.

57. **Roxo-Rosa M, Xu Z, Schmidt A, Neto M, Cai Z, Soares CM, Sheppard DN, Amaral MD.** Revertant mutants G550E and 4RK rescue cystic fibrosis mutants in the first nucleotide-binding domain of CFTR by different mechanisms. *Proc Natl Acad Sci USA* 103: 17891-17896, 2006.

58. **Sabusap CM, Wang W, McNicholas CM, Chung WJ, Fu L, Wen H, Mazur M, Kirk KL, Collawn JF, Hong JS, Sorscher EJ.** Analysis of cystic fibrosis-associated P67L CFTR illustrates barriers to personalized therapeutics for orphan diseases. *JCI Insight* 1: e86581, 2016.

59. **Sawicki GS, McKone EF, Pasta DJ, Millar SJ, Wagener JS, Johnson CA, Konstan MW.** Sustained benefit from ivacaftor demonstrated by combining clinical trial and cystic fibrosis patient registry data. *Am J Respir Crit Care Med* 192: 836-842, 2015.

60. **Schmidt A, Hughes LK, Cai Z, Mendes F, Li H, Sheppard DN, Amaral MD.** Prolonged treatment of cells with genistein modulates the expression and function of the cystic fibrosis transmembrane conductance regulator. *Br J Pharmacol* 153: 1311-1323, 2008.

61. **Sheppard DN, Robinson KA.** Mechanism of glibenclamide inhibition of cystic fibrosis transmembrane conductance regulator Cl^- channels expressed in a murine cell line. *J Physiol* 503: 333-346, 1997.

62. **Sorum B, Czégé D, Csanády L.** Timing of CFTR pore opening and structure of its transition state. *Cell* 163: 724-733, 2015.

63. **Szollosi A, Muallem DR, Csanády L, Vergani P.** Mutant cycles at CFTR's non-canonical ATP-binding site support little interface separation during gating. *J Gen Physiol* 137: 549-562, 2011.

64. **Traut TW.** Physiological concentrations of purines and pyrimidines. *Mol Cell Biochem* 140: 1-22, 1994.

65. **Tsai M-F, Li M, Hwang T-C.** Stable ATP binding mediated by a partial NBD dimer of the CFTR chloride channel. *J Gen Physiol* 135: 399-414, 2010.

66. **Turner MJ, Matthes E, Billet A, Ferguson AJ, Thomas DY, Randell SH, Ostrowski LE, Abbott-Banner K, Hanrahan JW.** The dual phosphodiesterase 3 and 4 inhibitor RPL554 stimulates CFTR and ciliary beating in primary cultures of bronchial epithelia. *Am J Physiol Lung Cell Mol Physiol* 310: L59-L70, 2016.

67. **Van Goor F, Hadida S, Grootenhuis PDJ, Burton B, Cao D, Neuberger T, Turnbull A, Singh A, Joubran J, Hazlewood A, Zhou J, McCartney J, Arumugam V, Decker C, Yang J, Young C, Olson ER, Wine JJ, Frizzell RA, Ashlock M,**

Negulescu P. Rescue of CF airway epithelial cell function in vitro by a CFTR potentiator, VX-770. *Proc Natl Acad Sci USA* 106: 18825-18830, 2009.

68. **Van Goor F, Hadida S, Grootenhuis PDJ, Burton B, Stack JH, Straley KS, Decker CJ, Miller M, McCartney J, Olson ER, Wine JJ, Frizzell RA, Ashlock M, Negulescu PA.** Correction of the F508del-CFTR protein processing defect in vitro by the investigational drug VX-809. *Proc Natl Acad Sci USA* 108: 18843-18848, 2011.

69. **Van Goor F, Yu H, Burton B, Hoffman BJ.** Effect of ivacaftor on CFTR forms with missense mutations associated with defects in protein processing or function. *J Cyst Fibros* 13: 29-36, 2014.

70. **Veit G, Avramescu RG, Chiang AN, Houck SA, Cai Z, Peters KW, Hong JS, Pollard HB, Guggino WB, Balch WE, Skach WR, Cutting GR, Frizzell RA, Sheppard DN, Cyr DM, Sorscher EJ, Brodsky JL, Lukacs GL.** From CFTR biology towards combinatorial pharmacotherapy: expanded classification of cystic fibrosis mutations. *Mol Biol Cell* 27: 424-433, 2016.

71. **Veit G, Avramescu RG, Perdomo D, Phuan P-W, Bagdany M, Apaja PM, Borot F, Szollosi D, Wu Y-S, Finkbeiner WE, Hegedus T, Verkman AS, Lukacs GL.** Some gating potentiators, including VX-770, diminish ΔF508-CFTR functional expression. *Sci Transl Med* 6: 246ra97, 2014.

72. **Venglarik CJ, Schultz BD, Frizzell RA, Bridges RJ.** ATP alters current fluctuations of cystic fibrosis transmembrane conductance regulator: evidence for a three-state activation mechanism. *J Gen Physiol* 104: 123-146, 1994.

73. **Vergani P, Lockless SW, Nairn AC, Gadsby DC.** CFTR channel opening by ATP-driven tight dimerization of its nucleotide-binding domains. *Nature* 433: 876-880, 2005.

74. **Vergani P, Nairn AC, Gadsby DC.** On the mechanism of MgATP-dependent gating of CFTR Cl^- channels. *J Gen Physiol* 121: 17-36, 2003.

75. **Wainwright CE, Elborn JS, Ramsey BW, Marigowda G, Huang X, Cipolli M, Colombo C, Davies JC, De Boeck K, Flume PA, Konstan MW, McColley SA, McCoy K, McKone EF, Munck A, Ratjen F, Rowe SM, Waltz D, Boyle MP, TRAFFIC and TRANSPORT Study Groups.** Lumacaftor-ivacaftor in patients with cystic fibrosis homozygous for Phe508del *CFTR*. *N Engl J Med* 373: 220-231, 2015.

76. **Wang W, Okeyo GO, Tao B, Hong JS, Kirk KL.** Thermally unstable gating of the most common cystic fibrosis mutant channel (ΔF508): "rescue" by suppressor mutations in nucleotide binding domain 1 and by constitutive mutations in the cytosolic loops. *J Biol Chem* 286: 41937-41948, 2011.

77. **Wang Y, Liu J, Loizidou A, Bugeja LA, Warner R, Hawley BR, Cai Z, Toye AM, Sheppard DN, Li H.** CFTR potentiators partially restore channel function to A561E-CFTR, a cystic fibrosis mutant with a similar mechanism of dysfunction as F508del-CFTR. *Br J Pharmacol* 171: 4490-4503, 2014.

78. **Yeh H-I, Yeh J-T, Hwang T-C.** Modulation of CFTR gating by permeant ions. *J Gen Physiol* 145: 47-60, 2015.

79. **Yu H, Burton B, Huang C-J, Worley J, Cao D, Johnson JP Jr, Urrutia A, Joubran J, Seepersaud S, Sussky K, Hoffman BJ, Van Goor F.** Ivacaftor potentiation of multiple CFTR channels with gating mutations. *J Cyst Fibros* 11: 237-245, 2012.

80. **Zhang Z, Chen J.** Atomic structure of the cystic fibrosis transmembrane conductance regulator. *Cell* 167: 1586-1597, 2016.

FIGURE LEGENDS

Figure 1: Temperature-dependence of wild-type and F508del-CFTR single-channel activity *A–C*: Representative recordings of wild-type and F508del-CFTR Cl^- channels in excised inside-out membrane patches from recombinant BHK cells. The plasma membrane expression of F508del-CFTR was rescued by either low temperature incubation (27 °C for 72 – 96 h) (*B*) or treatment with lumacaftor (VX-809; 3 μM) for 24 – 48 h at 37 °C (*C*). The recordings were acquired at the indicated temperatures in the presence of ATP (1 mM) and PKA (75 nM) in the intracellular solution. Dotted lines indicate where channels are closed and downward deflections correspond to channel openings. In this and subsequent figures, a large Cl^- concentration gradient was imposed across membrane patches ($[Cl^-]_{int}$, 147 mM; $[Cl^-]_{ext}$, 10 mM) and membrane voltage was clamped at –50 mV to magnify the size of channel openings.

Figure 2: Analysis of the temperature-dependence of wild-type and F508del-CFTR Cl^- channels *A–D*: Summary data show the change in single-channel current amplitude (i), open probability (P_o), mean burst duration (MBD) and interburst interval (IBI) between 23 and 37 °C for wild-type CFTR and F508del-CFTR rescued by either low temperature incubation (27 °C for 72 – 96 h) or lumacaftor (VX-809; 3 μM) for 24 – 48 h at 37 °C). Data are means ± SEM (wild-type, *A–B*, n = 5 – 9, *C–D*, n = 5 – 6; 27 °C-rescued F508del-CFTR, *A–B*, n = 5 – 13, *C–D*, n = 4 – 9; VX-809-rescued F508del-CFTR, *A–B*, n = 7 – 9, *C–D*, n = 5 – 8). In *A*, the continuous lines are the fit of first-order regression functions to mean data, whereas in *B–D*, they are the fit of second-order regression functions to mean data.

Figure 3: Temperature-dependence of wild-type and F508del-CFTR potentiation by the small molecule UC_{CF}-853 *A–C*: Representative recordings of wild-type and low

temperature-rescued F508del-CFTR Cl^- channels in excised inside-out membrane patches from recombinant BHK cells acquired at the indicated temperatures to show the effects of UC_{CF}-853 (P4; 10 μM) addition to the intracellular solution. For wild-type CFTR, ATP (0.3 mM) and PKA (75 nM) were continuously present in the intracellular solution, whereas for low temperature-rescued F508del-CFTR, ATP (1 mM) and PKA (75 nM) were used. For low temperature-rescued F508del-CFTR recordings acquired in the absence of P4, see Figure 1. Dotted lines indicate where channels are closed and downward deflections correspond to channel openings.

Figure 4: Analysis of the temperature-dependence of wild-type and F508del-CFTR potentiation by UC_{CF}-853 *A–D*: Summary data show the change in single-channel current amplitude (i), open probability (P_o), mean burst duration (MBD) and interburst interval (IBI) between 23 and 37 °C for wild-type and low temperature-rescued F508del-CFTR in the absence and presence of UC_{CF}-853 (P4; 10 μM) in the intracellular solution. Data are means ± SEM (wild-type, *A–B*, n = 5 – 8, *C–D*, n = 4 – 5; 27 °C-rescued F508del-CFTR, *A–B*, n = 4 – 8, *C–D*, n = 3 – 5). In *A*, the continuous lines are the fit of first-order regression functions to mean data, whereas in *B–D*, they are the fit of second-order regression functions to mean data.

Figure 5: The effects of temperature on wild-type and F508del-CFTR potentiation by ivacaftor *A* and *B*: Representative recordings of wild-type CFTR and low temperature-rescued F508del-CFTR in excised inside-out membrane patches from recombinant BHK cells acquired at the indicated temperatures to show the effects of acute addition of ivacaftor (VX-770; 10 μM) to the intracellular solution. For wild-type CFTR, ATP (0.3 mM) and PKA (75 nM) were continuously present in the intracellular solution, whereas for F508del-CFTR, ATP

(1 mM) and PKA (75 nM) were used. For control recordings acquired in the absence of ivacaftor, see Figure 3 for wild-type CFTR and Figure 1 for low temperature-rescued F508del-CFTR. Dotted lines indicate where channels are closed and downward deflections correspond to channel openings.

Figure 6: Analysis of the temperature-dependence of wild-type and F508del-CFTR potentiation by ivacaftor *A–D*: Summary data show the change in single-channel current amplitude (i), open probability (P_o), mean burst duration (MBD) and interburst interval (IBI) between 23 and 37 °C for wild-type and low temperature-rescued F508del-CFTR in the absence and presence of ivacaftor (VX-770; 10 μM) added acutely to the intracellular solution. Data are means ± SEM (wild-type, *A–B*, n = 5 – 7, *C–D*, n = 4 – 6; 27 °C-rescued F508del-CFTR, n = 4 – 7). In *A*, the continuous lines are the fit of first-order regression functions to mean data, whereas in *B–D*, they are the fit of second-order regression functions to mean data.

Figure 7: The temperature-dependence of F508del-CFTR potentiated by nanomolar concentrations of ivacaftor *A*: Representative recordings of low temperature-rescued F508del-CFTR in an inside-out membrane patch excised from a recombinant BHK cell acquired at the indicated temperatures to show the effects of acute addition of ivacaftor (VX-770; 100 nM) to the intracellular solution. The recordings were made in the continuous presence of ATP (1 mM) and PKA (75 nM) in the intracellular solution. For control recordings acquired in the absence of ivacaftor, see Figure 1. Dotted lines indicate where channels are closed and downward deflections correspond to channel openings. *B–E*: Summary data show the change in single-channel current amplitude (i), open probability (P_o), mean burst duration (MBD) and interburst interval (IBI) between 23 and 37 °C for low

temperature-rescued F508del-CFTR potentiated by ivacaftor (VX-770; 100 nM). Data are means ± SEM (*B–C*, n = 4 – 5; *D–E*, n = 3 – 4). In *B* and *C*, the continuous lines are the fit of first-order regression functions to mean data, whereas in *D* and *E*, they are the fit of second-order regression functions to mean data. For control data acquired in the absence of ivacaftor, see Figure 6.

Figure 8: Potentiation of lumacaftor-rescued F508del-CFTR Cl^- channels by chronic treatment with ivacaftor *A* and *B*: Representative recordings of wild-type and F508del-CFTR rescued by either low temperature incubation or treatment with lumacaftor (VX-809; 3 μM) in excised inside-out membrane patches from recombinant BHK cells acquired at either 27 °C (*A*) or 37 °C (*B*) to show the effects of acute (aVX-770; 10 μM) and chronic (cVX-770; 1 μM) ivacaftor treatment. ATP (1 mM) and PKA (75 nM) were continuously present in the intracellular solution. Dotted lines indicate where channels are closed and downward deflections correspond to channel openings.

Figure 9: Chronic ivacaftor potentiates robustly lumacaftor-rescued F508del-CFTR Cl^- channels at 27 and 37 °C *A–D*: Summary data show the single-channel current amplitude (i), open probability (P_o), mean burst duration (MBD) and interburst interval (IBI) at 27 and 37 °C for wild-type CFTR and lumacaftor (VX-809)-rescued F508del-CFTR treated either acutely (aVX-770; 10 μM) or chronically (cVX-770; 1 μM) with ivacaftor. Data are means ± SEM (wild-type: *A–B*, n = 6 – 10, *C–D*, n = 6; 27 °C-rescued F508del-CFTR: control, *A–B*, n = 10 – 14, *C–D*, n = 9; aVX-770, *A–B*, n = 4 – 5, *C–D*, n = 4; VX-809-rescued F508del-CFTR: control *A–B*, n = 7 – 8, *C–D*, n = 5 – 6; aVX-770, *A–B*, n = 4 – 8, *C–D*, n = 4 – 6; cVX-770, *A–B*, n = 9 – 10, *C–D*, n = 4 – 5); *, $P < 0.05$ vs. wild-type CFTR; †, $P < 0.05$ vs. F508del-CFTR; ‡, $P < 0.05$ vs. F508del-CFTR, VX-809.

968

TABLES

Table 1: Temperature coefficients of wild-type and F508del-CFTR

Conditions	Temperature coefficient (Q_{10}) values		
	i	Opening rate (1/IBI)	Closing rate (1/MBD)
WT CFTR (1 mM ATP)	1.39 ± 0.04	4.73 ± 1.14	1.47 ± 0.11*
WT CFTR (0.3 mM ATP)	1.37 ± 0.05	3.95 ± 0.79	1.50 ± 0.18*
WT CFTR (0.3 mM ATP + P4)	1.35 ± 0.03	4.46 ± 0.88	1.11 ± 0.09
WT CFTR (0.3 mM ATP + VX-770)	1.39 ± 0.02	1.89 ± 0.26	1.75 ± 0.12
F508del-CFTR; 27 °C-rescued	1.53 ± 0.03	5.24	3.36
F508del-CFTR; VX-809-rescued	1.54 ± 0.05	5.38 ± 1.35	3.24 ± 0.33
F508del-CFTR; 27 °C-rescued; P4	1.35 ± 0.04	4.45	1.60
F508del-CFTR; 27 °C-rescued; VX-770 (10 μM)	1.50 ± 0.06	3.45 ± 0.98	3.63 ± 0.62
F508del-CFTR; 27 °C-rescued; VX-770 (100 nM)	1.30 ± 0.02	3.20 ± 0.45	2.60 ± 0.67

Temperature coefficient (Q_{10}) values for single-channel current amplitude (i), channel opening rate and channel closing rate of wild-type and F508del-CFTR calculated from mean values of single-channel current amplitude, IBI and MBD for the indicated experimental conditions; UC_{CF}-853 was tested at 10 μM and ivacaftor at 100 nM (F508del-CFTR only) or 10 μM. Data are means ± SEM (n = 4, except wild-type CFTR (0.3 and 1 mM ATP) and VX-809-rescued F508del-CFTR, where n= 5); *, $P < 0.05$ vs. opening rate. For low temperature-rescued F508del-CFTR in the absence and presence of UC_{CF}-853, channel deactivation at 37 °C prevented collection of sufficient data to determine Q_{10} values for opening and closing rates. Abbreviations: P4, UC_{CF}-853; VX-770, ivacaftor; VX-809, lumacaftor.

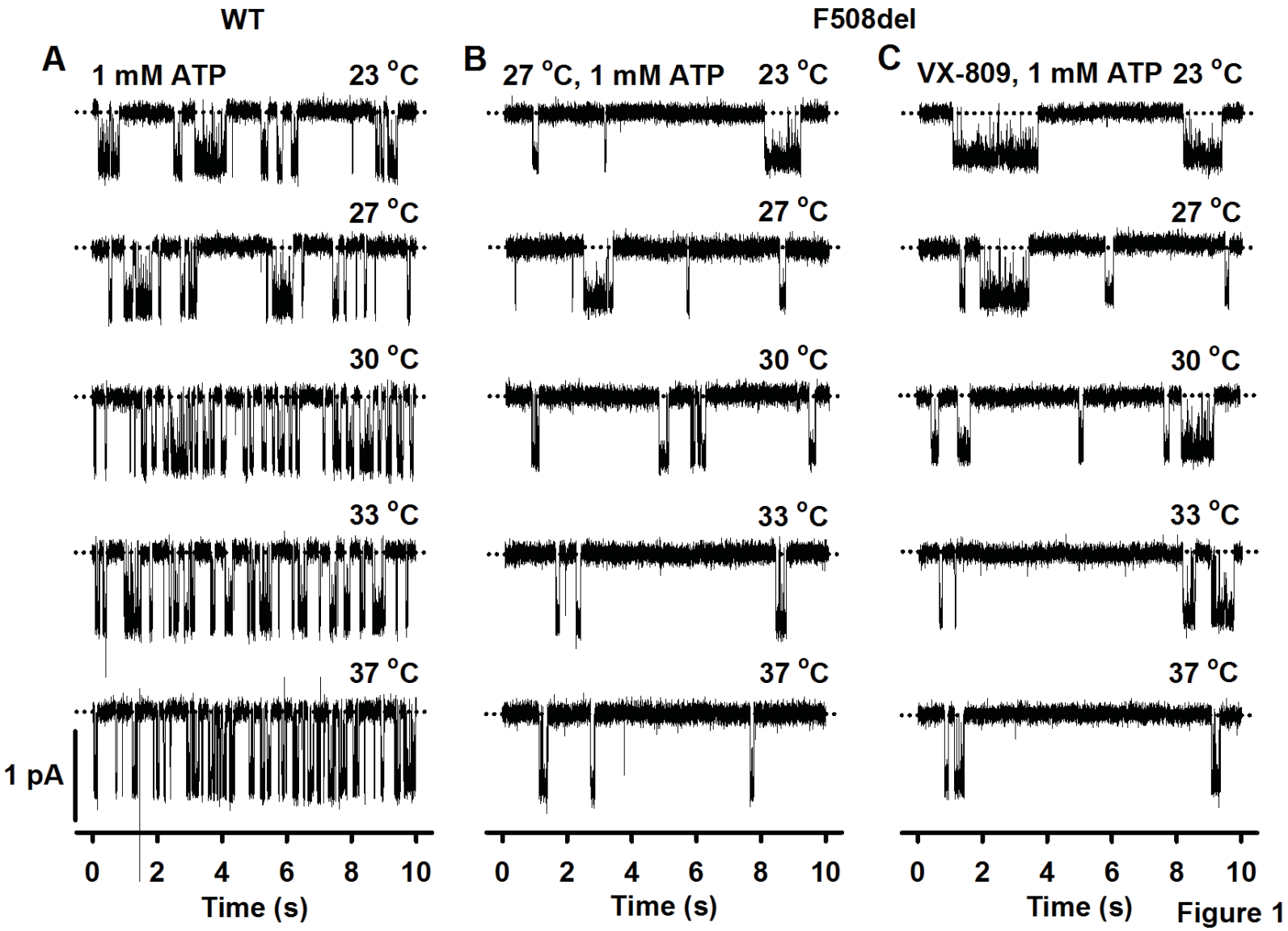
WT
F508del
A
1 mM ATP
23 °C
27 °C
30 °C
33 °C
37 °C
1 pA
0
2
4
6
8
10
Time (s)
B
27 °C, 1 mM ATP
23 °C
27 °C
30 °C
33 °C
37 °C
0
2
4
6
8
10
Time (s)
C
VX-809, 1 mM ATP
23 °C
27 °C
30 °C
33 °C
37 °C
0
2
4
6
8
10
Time (s)

Figure 1

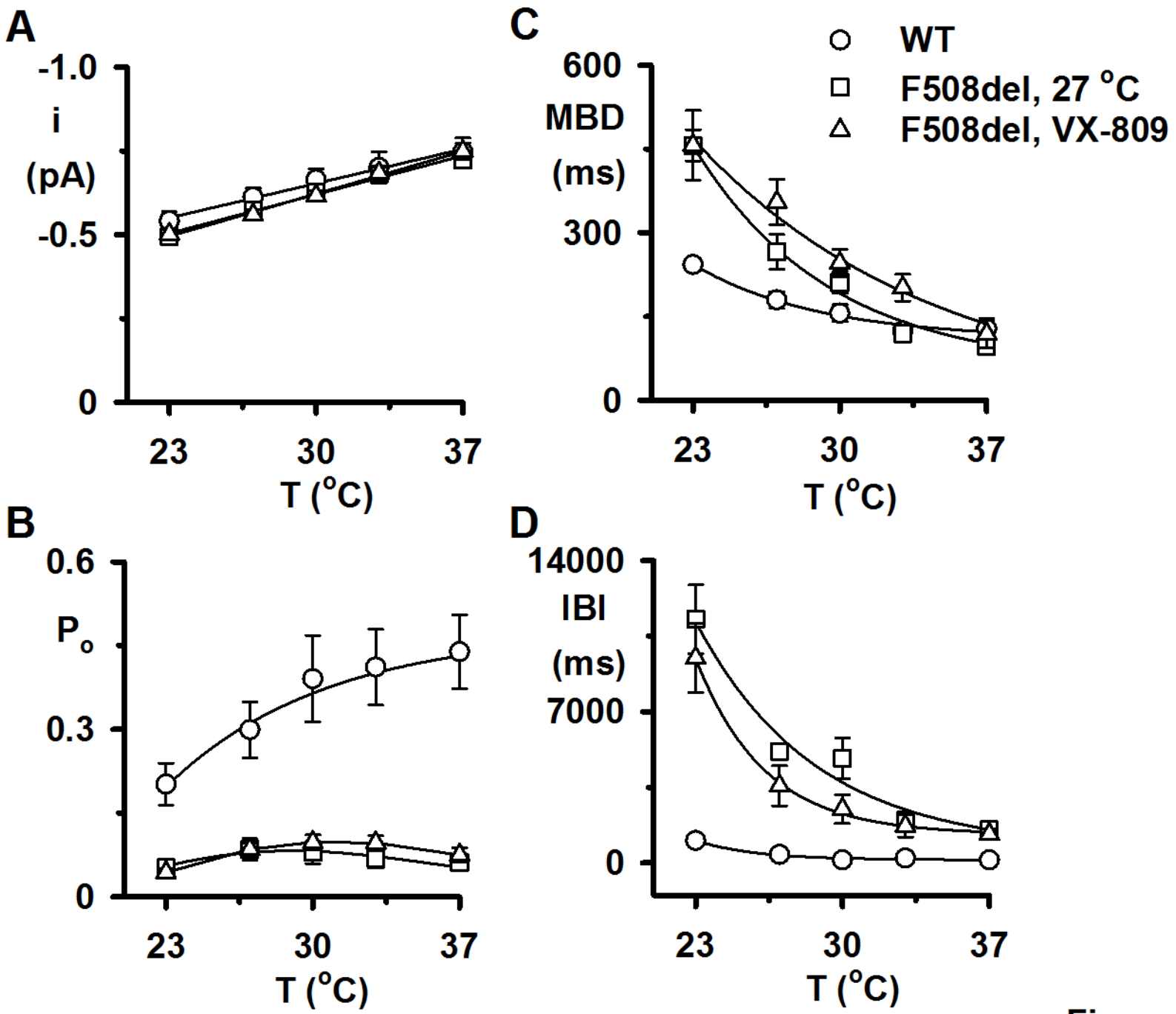
A
-1.0
i
(pA)
-0.5
0
23
30
37
T (°C)
C
600
MBD
(ms)
300
0
WT
F508del, 27 °C
F508del, VX-809
B
0.6
P_o
0.3
D
14000
IBI
(ms)
7000

Figure 2

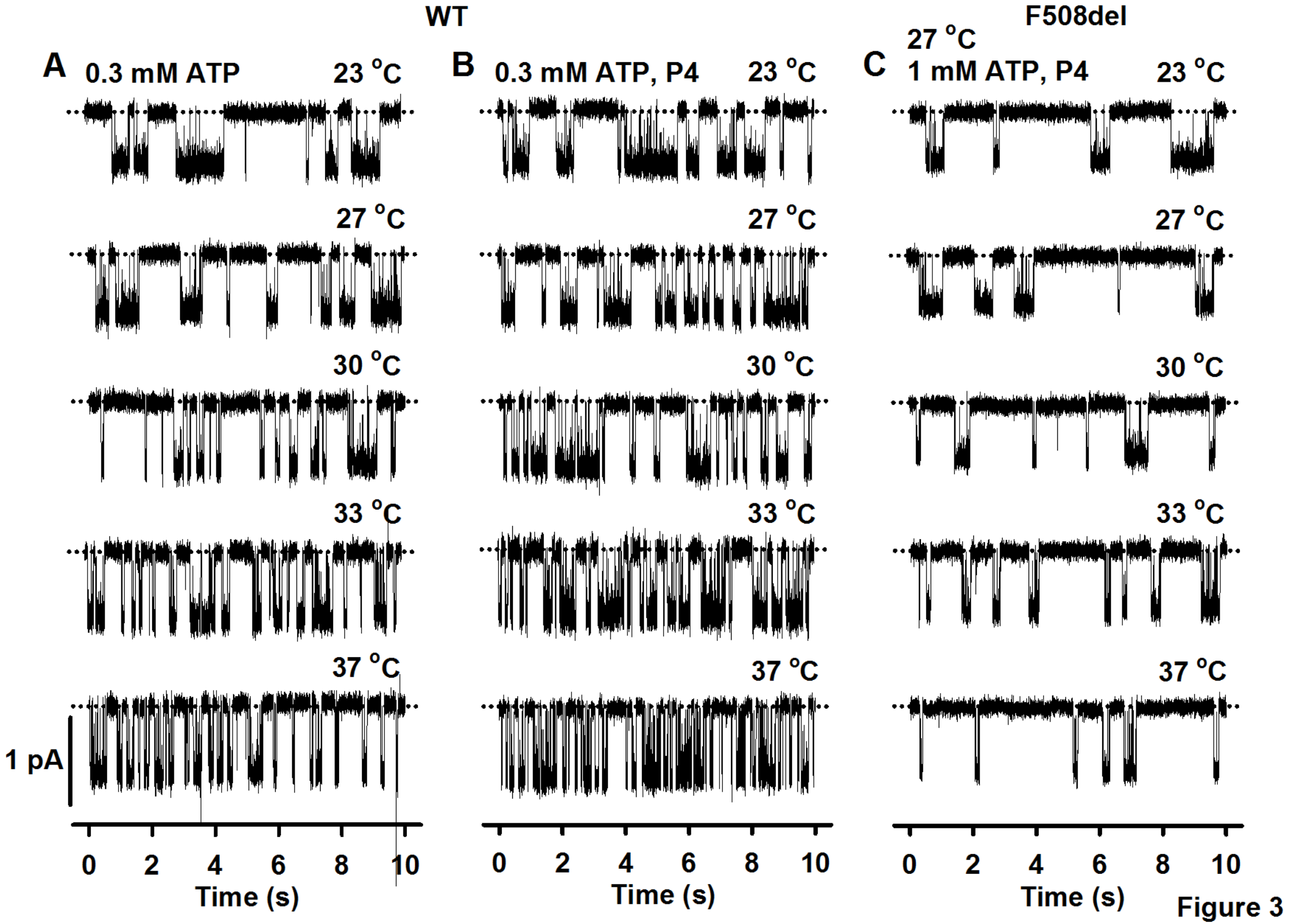
WT
F508del
A
0.3 mM ATP
23 °C
27 °C
30 °C
33 °C
37 °C
B
0.3 mM ATP, P4
23 °C
27 °C
30 °C
33 °C
37 °C
C
27 °C
1 mM ATP, P4
23 °C
27 °C
30 °C
33 °C
37 °C
1 pA
0
2
4
6
8
10
Time (s)
0
2
4
6
8
10
Time (s)
0
2
4
6
8
10
Time (s)

Figure 3

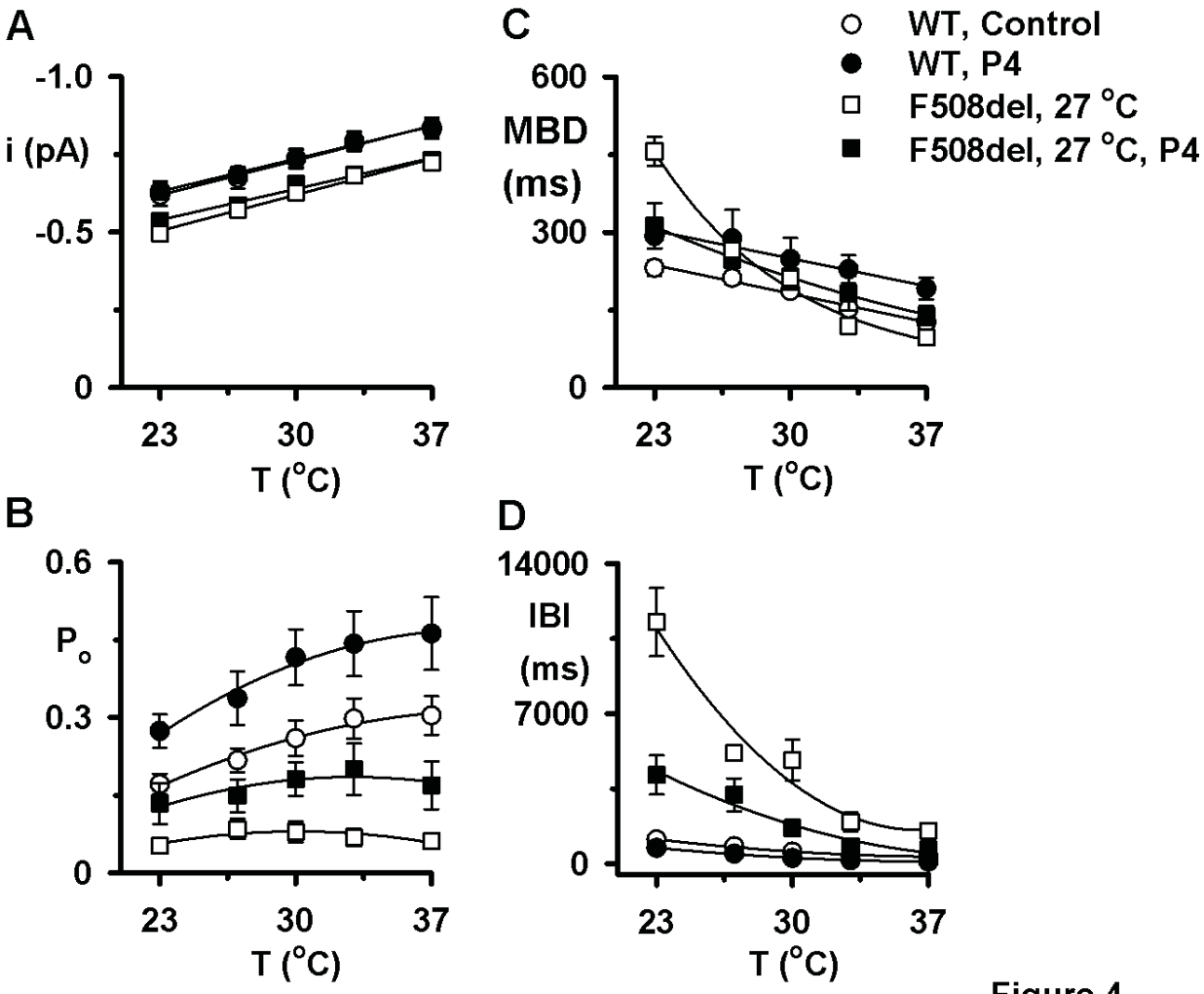
A
-1.0
i (pA)
-0.5
0
23
30
37
T (°C)
C
600
MBD
(ms)
300
0
23
30
37
T (°C)
WT, Control
WT, P4
F508del, 27 °C
F508del, 27 °C, P4
B
0.6
P_o
0.3
0
23
30
37
T (°C)
D
14000
IBI
(ms)
7000
0
23
30
37
T (°C)

Figure 4

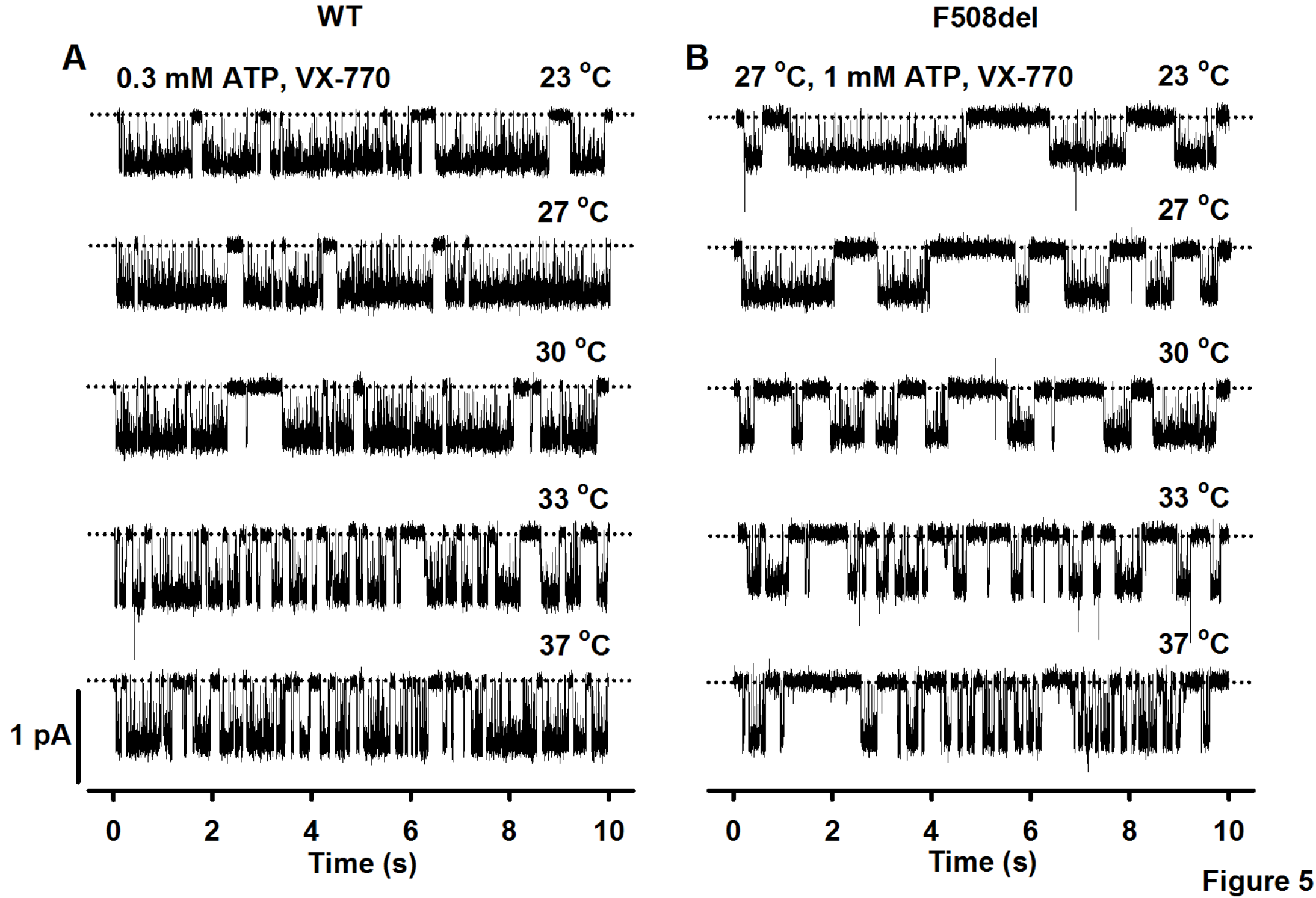
WT
F508del
A
0.3 mM ATP, VX-770
23 °C
27 °C
30 °C
33 °C
37 °C
1 pA
0
2
4
6
8
10
Time (s)
B
27 °C, 1 mM ATP, VX-770
23 °C
27 °C
30 °C
33 °C
37 °C
0
2
4
6
8
10
Time (s)

Figure 5

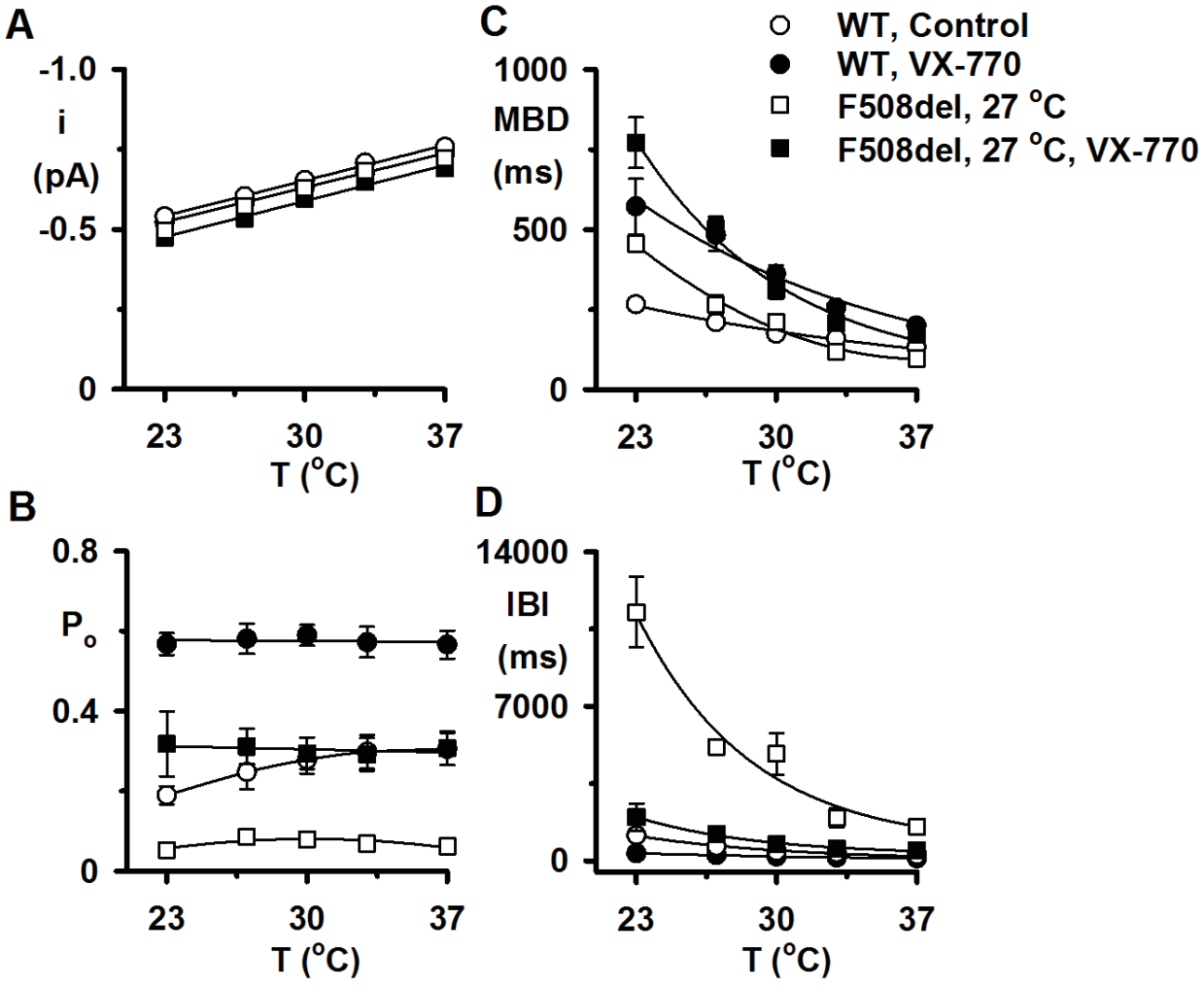
A
-1.0
i
(pA)
-0.5
0
23
30
37
T (°C)
C
1000
MBD
(ms)
500
0
23
30
37
T (°C)
WT, Control
WT, VX-770
F508del, 27 °C
F508del, 27 °C, VX-770
B
0.8
P_o
0.4
0
23
30
37
T (°C)
D
14000
IBI
(ms)
7000
0
23
30
37
T (°C)

Figure 6

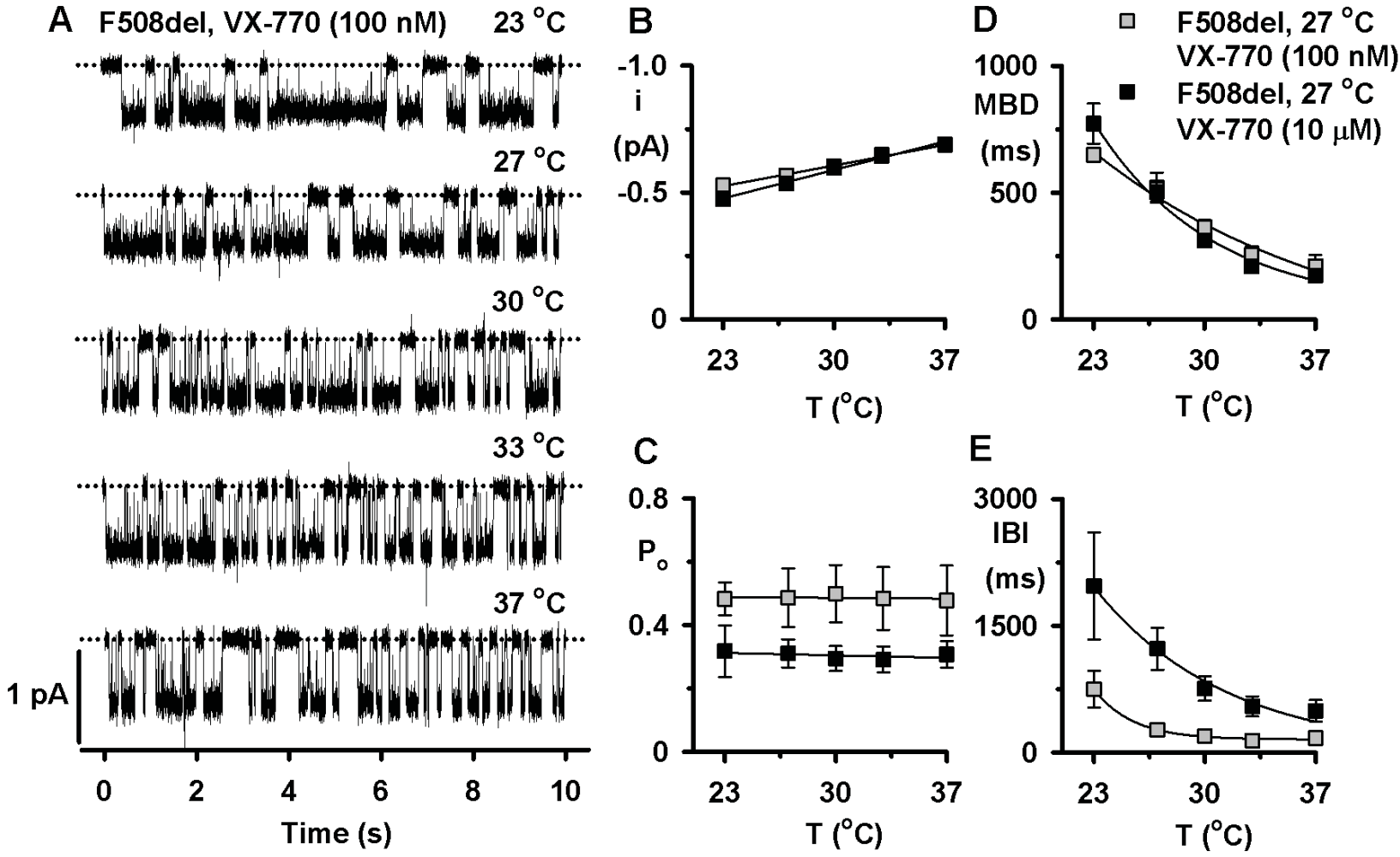
A
F508del, VX-770 (100 nM)
23 °C
27 °C
30 °C
33 °C
37 °C
1 pA
0
2
4
6
8
10
Time (s)
B
-1.0
i
(pA)
-0.5
0
23
30
37
T (°C)
C
0.8
P
o
0.4
0
23
30
37
T (°C)
D
F508del, 27 °C
VX-770 (100 nM)
F508del, 27 °C
VX-770 (10 μM)
1000
MBD
(ms)
500
0
23
30
37
T (°C)
E
3000
IBI
(ms)
1500
0
23
30
37
T (°C)

Figure 7

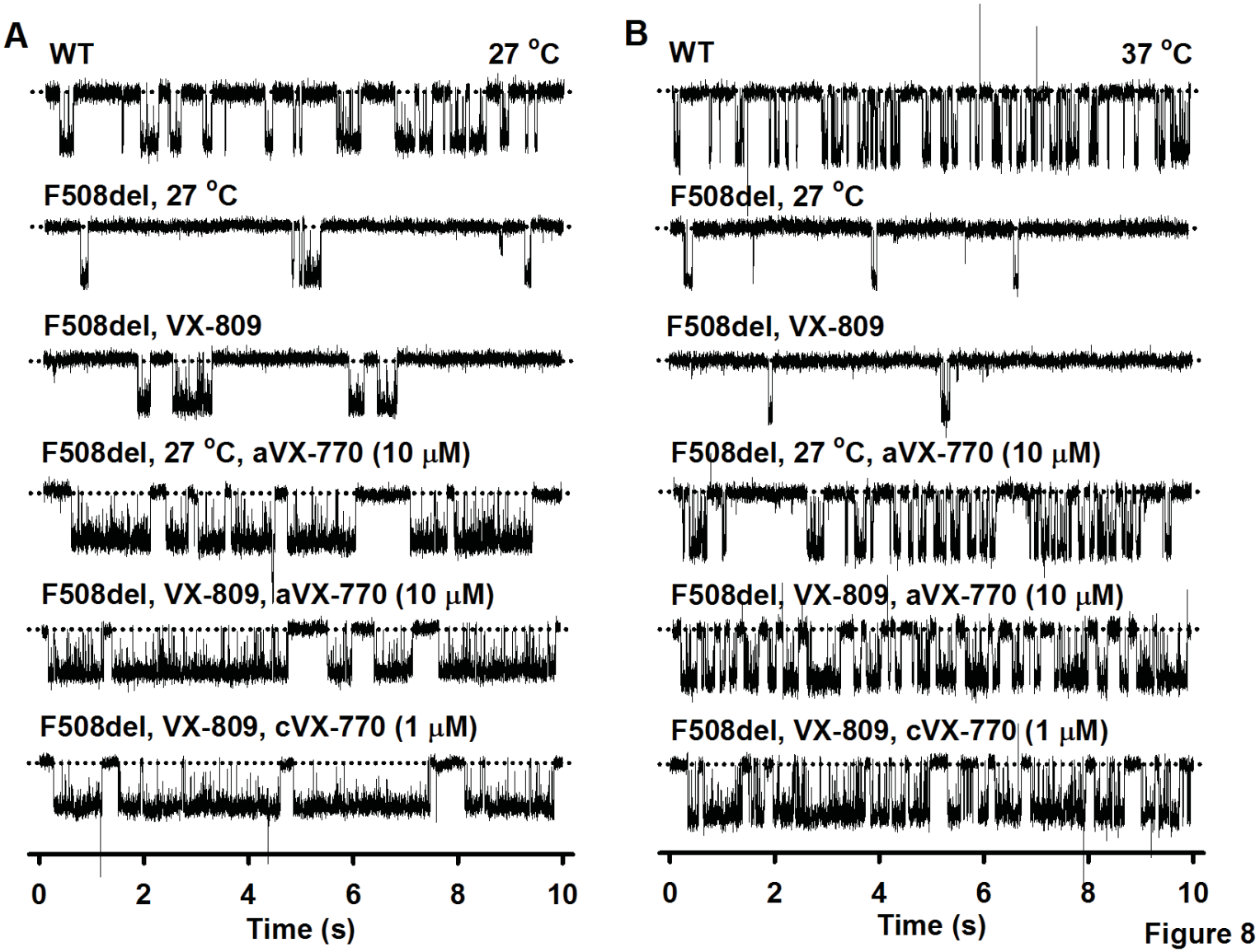
A
WT
27 °C
F508del, 27 °C
F508del, VX-809
F508del, 27 °C, aVX-770 (10 μM)
F508del, VX-809, aVX-770 (10 μM)
F508del, VX-809, cVX-770 (1 μM)
0
2
4
6
8
10
Time (s)
B
WT
37 °C
F508del, 27 °C
F508del, VX-809
F508del, 27 °C, aVX-770 (10 μM)
F508del, VX-809, aVX-770 (10 μM)
F508del, VX-809, cVX-770 (1 μM)
0
2
4
6
8
10
Time (s)

Figure 8

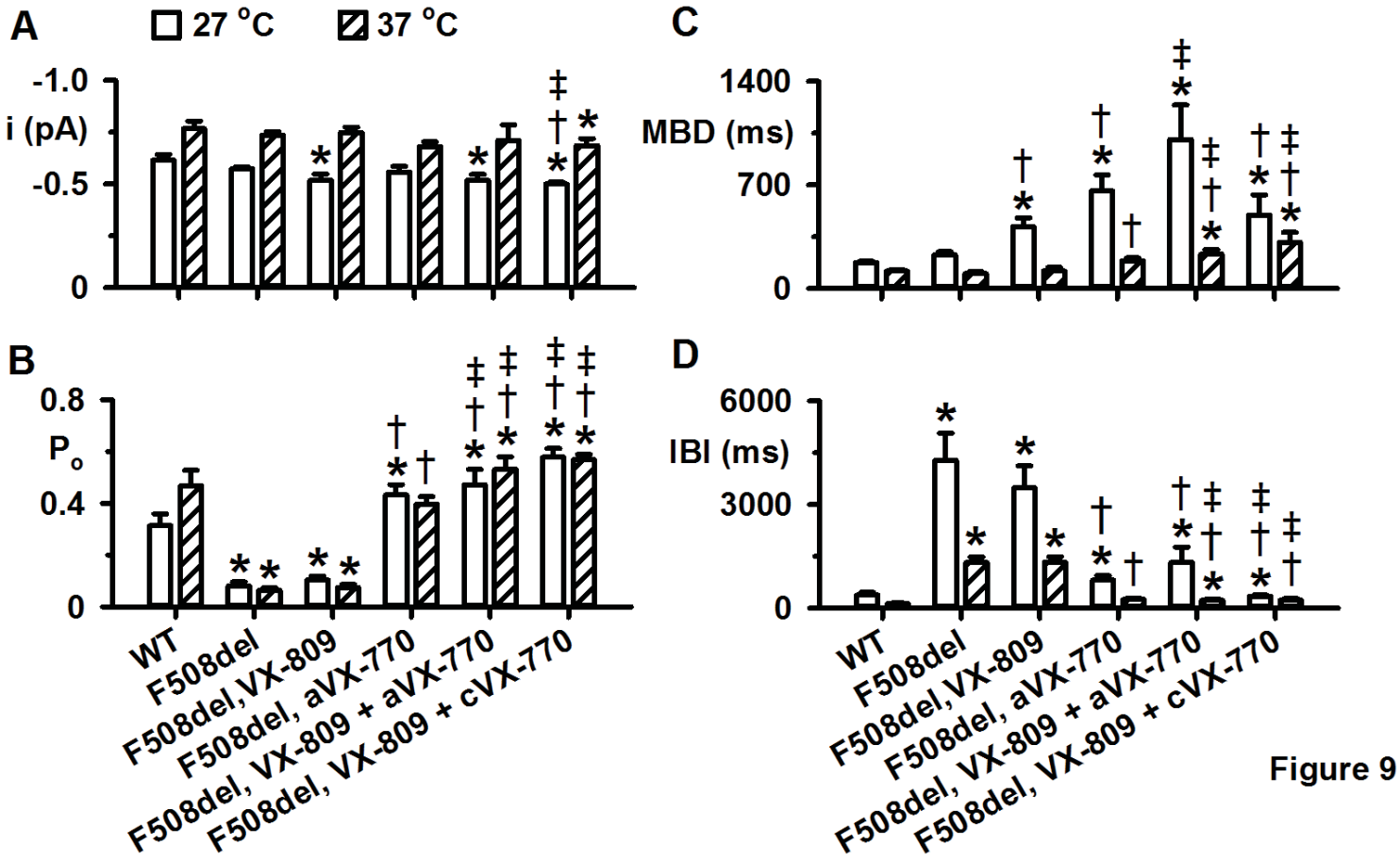
A
27 °C
37 °C
-1.0
i (pA)
-0.5
0
B
0.8
Po
0.4
0
C
1400
MBD (ms)
700
0
D
6000
IBI (ms)
3000
0
WT
F508del
F508del,VX-809
F508del, aVX-770
F508del, VX-809 + aVX-770
F508del, VX-809 + cVX-770

Figure 9